

USER COOPERATIVE COMMUNICATIONS IN ULTRA-WIDEBAND
WIRELESS NETWORKS

by

Cumhur Ozan Yalçın

B.S., in Electrical and Electronics Engineering, Bogazici University, 2005

Submitted to the Institute for Graduate Studies in
Science and Engineering in partial fulfillment of
the requirements for the degree of
Master of Science

Graduate Program in Electrical and Electronics Engineering
Boğaziçi University

2008

To My Family...

ACKNOWLEDGEMENTS

I would like to express my gratitude to Assist. Prof. Mutlu Koca for his guidance and help during the preparation of this thesis. I would like to mention his patience when I stuck at dead-ends.

I am also very thankful to my family for their infinite support and trust on me. They always encouraged me to complete my M.S. degree.

I am grateful to my best friends Orkun Sağlamdemir, Ömer Yetik, Yücel Altuğ and Polat Ayerden for their support. I've easily got rid of stress during times spent together.

I would like to thank to my friends Barış Özgül, Nazlı Güney, Ersen Ekrem and Salim Bahçeci in Wireless Communications Laboratory for friendship, useful discussions and help.

This thesis has been supported by TUBITAK (Scientific and Technological Research Council of Turkey) Research Grant under Contract 105E077.

ABSTRACT

USER COOPERATIVE COMMUNICATIONS IN ULTRA-WIDEBAND WIRELESS NETWORKS

In this thesis, we consider the user cooperation in ultra-wideband (UWB) systems characterized by severe frequency selective channels. To circumvent this problem we present a space-time (ST) coded UWB system employing the multiband orthogonal frequency division multiplexing (MB-OFDM). Space-time coded cooperation (STCC) is subject to error floors due to hard-decision detection errors in between users. For this reason we propose a soft-information aided cooperation mechanism which lower the error floor significantly. Adding iterative decoding to partners improved the performance further. We also proposed a cyclic redundancy check (CRC) employed system to decide on cooperation. The simulation results and comparisons with the single user case indicate that the proposed user cooperative UWB transceiver architectures have significantly improved error floor and bit-error rate (BER) performance.

ÖZET

ÇOK GENİŞ BANTLI TELSİZ İLETİŞİM AĞLARINDA KULLANICI İŞBİRLİKLİ HABERLEŞME

Bu tezde, seçici sönümlenmeden çok etkilenen Çok Geniş Bantlı (ÇGB) sistemler için kullanıcı işbirlikli haberleşme teknikleri üzerine çalışılmıştır. Bu problemi çözebilmek için Çok Bantlı Dikgen Frekans Bölüşümlü Çoğullamadan faydalanan Uzay-Zaman Kodlamalı (UZK) ÇGB sistemi kullanılmıştır. UZK işbirliği performansı, kullanıcılardaki sıfır-bir kararlarından doğan hatalar sebebiyle hata sınırıyla sınırlanır. Bu sebeple, bu hata sınırını aşağıya çekmek için yumuşak karar kullanan işbirliği tekniği önerilmiştir. Yardımlaşan kullanıcılarda özyineli çözümleme kullanmak performansı daha da iyileştirmiştir. Bunlara ek olarak, Çevrimsel Artıklık Kodu (ÇAK) kullanılarak işbirliğine karar veren bir sistemle de hata sınırını ortadan kaldırmak mümkün olmuştur. Kuramsal çözümler ve benzetim sonuçlarının tek kullanıcıli sistemle karşılaştırılması, önerilen kullanıcı işbirlikli ÇGB alıcı-verici yapılarının hata sınırını aşağı çektiğini ve bit hata oranını iyileştirdiğini göstermiştir.

TABLE OF CONTENTS

ACKNOWLEDGEMENTS	iv
ABSTRACT	v
ÖZET	vi
LIST OF FIGURES	viii
LIST OF TABLES	x
LIST OF SYMBOLS/ABBREVIATIONS	xi
1. INTRODUCTION	1
2. COOPERATIVE DIVERSITY	3
2.1. Diversity	3
2.2. Cooperation	6
3. SPACE-TIME CODING	12
4. CONVOLUTIONAL CODING AND MAP DECODING	21
4.1. Decoding of Convolutional Codes	23
4.1.1. MAP Algorithm for Rate $1/n$ Convolutional Codes with AWGN Channel	23
4.2. Iterative Decoding	27
5. MULTIBAND OFDM ULTRA WIDEBAND SYSTEM	30
6. SPACE TIME CODED UWB COOPERATION	34
6.1. Cooperation with Soft Decoding	37
6.2. Cooperation with Iterative Decoding	38
6.3. Cooperation with CRC	38
7. ERROR PERFORMANCE ANALYSIS	40
7.1. Performance of User Cooperative MB-OFDM without CRC	40
7.2. Performance of User Cooperative MB-OFDM with CRC	41
8. SIMULATIONS AND RESULTS	44
9. CONCLUSIONS	48
APPENDIX A: DERIVATION OF EXTRINSIC LLR IN EQUATION 4.21	49
APPENDIX B: DERIVATION OF EQUATION 7.5	50
REFERENCES	52

LIST OF FIGURES

Figure 2.1.	Space diversity with multiple transmit and receive antennas.	4
Figure 2.2.	Cooperation model of Sendonaris <i>et al.</i>	8
Figure 2.3.	Cooperative transmission model of LEACH [3]. ● : primary heads, △ : secondary heads.	10
Figure 3.1.	The BER performance comparison of coherent BPSK with maximal ratio receiver combining (MRRC) and two-branch transmit diversity in Rayleigh fading [1].	15
Figure 3.2.	The BER performance comparison of space-time coded communications at 2bits/s/Hz rate with different number of transmit antennas and one receive antenna.	19
Figure 4.1.	Rate 1/2 binary nonsystematic feedforward convolutional encoder with memory order m=3.	22
Figure 4.2.	A sample trellis diagram with 1 input and 2 output bits.	23
Figure 4.3.	Iterative decoding system.	27
Figure 4.4.	Example EXIT chart for iterative decoding system.	28
Figure 4.5.	Iterative decoding performance of MB OFDM system.	29
Figure 5.1.	MB OFDM system model proposed in [35].	30
Figure 5.2.	Cyclic prefix and the OFDM symbol.	31

Figure 6.1.	Two user cooperation model.	34
Figure 6.2.	STCC with iterative decoding system model.	39
Figure 7.1.	Theoretical BER for uncoded STCC schemes at 20dB CM1 inter-user channel.	42
Figure 7.2.	Theoretical BER for uncoded STCC schemes symmetrical channel conditions in between users and destination.	43
Figure 8.1.	Simulation results for proposed ST coded MB OFDM cooperation scenarios with 20dB inter-user SNR.	44
Figure 8.2.	Simulation results for proposed ST coded MB OFDM cooperation scenarios with 10dB inter-user SNR.	45
Figure 8.3.	Simulation results of proposed ST coded MB-OFDM cooperation systems in symmetrical channel conditions.	46
Figure 8.4.	Simulation results for STCC-ID with and without CRC at 20dB inter-user SNR.	47
Figure 8.5.	Simulation results for STCC-ID at 20dB CM1 inter-user SNR. The user-destination channel is CM3.	47

LIST OF TABLES

Table 6.1.	Probability distribution of inter-user symbol error e	36
------------	---	----

LIST OF SYMBOLS/ABBREVIATIONS

B	Input for IFFT
c	Output of convolutional encoder
$c_{k,l}$	l^{th} code-bit of k^{th} element of c
$\bar{c}_{k,l}$	Soft bit for $c_{k,l}$
E_b	Energy per bit
e	Hard decision error on QPSK symbol at partner
e'	Soft decision error on QPSK symbol at partner
F	Fourier transform matrix
h	Discrete-time baseband channel impulse response
$h_i(t)$	Time-domain impulse response of i^{th} realization of channel
H	Circulant matrix generated from h
L	Length of $h[n]$
L_{cp}	Length of cyclic prefix
L_g	Length of guard interval
L_u	Length of information data stream u
$L(c_{k,l})$	Log-likelihood ratio of code-bit $c_{k,l}$
$L_a(c_{k,l})$	<i>A priori</i> log-likelihood ratio
$L_e(c_{k,l})$	Extrinsic log-likelihood ratio
N	Length of FFT
N	Frequency-domain noise sequence
N_b	Length of a frame
N_0	Noise power
P_b	Bit error probability of inter-user channel
P_e^{2x1}	Bit error rate of uncoded 2x1 system
P_e^{STCC}	Bit error rate of uncoded STCC system
P_e^{CRC}	Bit error rate of uncoded STCC system with CRC
P_f	Frame error rate of inter-user channel
P_e^{SU}	Bit error rate of single user system
S	QPSK symbol sequence

\hat{S}	Estimate of S
S_k	k^{th} element of S
\tilde{S}_i	Hard decision on symbol S_i at partner
\bar{S}	Soft symbol decision of S
T_l^i	Delay of l^{th} cluster of in i^{th} realization of channel
u	Information data stream
u_i	i^{th} element of u
x	Output of IFFT
\tilde{x}	Transmitted baseband signal
Y	Received frequency-domain information symbol sequence
\tilde{y}	Received baseband signal
\bar{y}	Received signal after removing cyclic prefix and guard interval
\bar{Y}	FFT of \bar{y}
α	Magnitude-square of fading coefficient affecting a symbol through user-1 to destination
β	Magnitude-square of fading coefficient affecting a symbol through user-2 to destination
$\alpha_{k,l}^i$	Multipath gain coefficient of the k -th multipath component within the l -th cluster of i^{th} realization of channel
χ	Log-normal shadowing coefficient
$\tilde{\eta}[n]$	Complex additive white Gaussian noise
σ_x^2	Variance of random variable x
γ	Signal-to-Noise Ratio E_b/N_0
$\bar{\gamma}$	Mean of $ \Lambda_{ij} ^2$
$\bar{\Lambda}$	Diagonal matrix with FFT coefficients of h
Λ_{ij}	FFT coefficients of channels from user j to destination at time slot i
$\tau_{k,l}^i$	Delay of the k -th multipath component within the l -th cluster
AWGN	Additive White Gaussian Noise
BER	Bit Error Rate

BPSK	Binary Phase Shift Keying
CP	Cyclic Prefix
CRC	Cyclic Redundancy Check
CSI	Channel State Information
FFT	Fast Fourier Transform
GI	Guard Interval
IFFT	Inverse Fast Fourier Transform
ISI	Inter-symbol Interference
LLR	Log-Likelihood Ratio
MAP	Maximum A posteriori Probability
MB-OFDM	Multiband Orthogonal Frequency Division Multiplexing
MIMO	Multiple Input Multiple Output
MGF	Moment Generating Function
OFDM	Orthogonal Frequency Division Multiplexing
QPSK	Quadrature Phase Shift Keying
SNR	Signal-to-Noise Ratio
ST	Space-Time
STC	Space-Time Coding
STBC	Space-Time Block Coding
STCC	Space-Time Coded Cooperation
SU	Single User
S-V	Saleh-Valenzuela
UWB	Ultra Wideband

1. INTRODUCTION

During a wireless data transmission, the transmitted signals suffer from fading. The fading is a random process which causes severe variations in signal attenuation. Diversity, which is sending the coded copies of signal through different channels, is an effective way to combat with fading [1]. In general, this is performed by using multiple antennas at the transmitter.

Placing multiple antennas on small mobile nodes is impractical because of spatial constraints. So we need to introduce new techniques to implement spatial diversity on mobile networks. User cooperative diversity aims to achieve spatial diversity without the need to use of multiple antennas especially when the size of the user terminals does not allow the use of more than one antenna. As proposed in [2, 3] one way to do this is to employ the explicit cooperation of a relay which does not have data to transmit. Another method proposed in [4] and [5] for a user is to utilize other user(s) as the relay(s) and to transmit both its own data and the neighboring data. Results in these works show that systems based on user cooperation achieve gains close to that of the multiantenna systems when the interuser channels are flat fading or perfect. However in the case where the interuser channels are frequency selective, user cooperation is possible with the use of orthogonal frequency division multiplexing (OFDM) where a cyclic prefix is added to the transmitted data blocks and the channel per tone is observed as flat-fading. For example, we refer to [6] and [7] which employ coded cooperation and distributed ST coded cooperation with OFDM, respectively.

In ultra-wideband communication (UWB) systems, the operation frequencies and the size of the devices prevents the use of multiple antennas. Therefore user cooperative diversity can be used in UWB systems to achieve the spatial diversity and to obtain the gains of space-time or space-frequency codes. For this reason we consider a 2-user cooperative diversity in space-time coded UWB systems and propose an effective cooperation scheme. Because the UWB channels are characterized by severe frequency selective fading as shown in [8], multiband OFDM (MB-OFDM) is employed

to implement the UWB transmission instead of an impulse radio structure.

In a ST coded 2-user cooperation scheme, the users transmit their information symbols to the base station in the first transmission period. During this period they also detect their partner's information. In the second transmission interval, each transmits the detected symbol of its partner using the Alamouti code [1]. However the hard decision errors in between users limit the overall system and cause an error floor in receiver error performance as shown in [9]. That is why we propose a soft cooperation mechanism where each user employs a soft-input soft-output detector to generate log likelihood decisions similar to that proposed in [10]. Our work is novel in that we applied ST cooperation into UWB systems and the soft user cooperation is combined with space-time coding. It is shown that the soft information exchange in between users reduces the error floor significantly. Furthermore as shown in the simulation results turbo processing can also be employed at the users, introducing further gains in performance after only a few iterations. We also use a CRC check employed scenario in which partners decide to cooperate or not according to CRC. This scheme allows us to get rid of error floor where single user performance outperforms erroneous cooperation.

This thesis is organized as follows. In Chapter 2, we will give the details of diversity and cooperation. Space-time coding is explained in Chapter 3. We represent convolutional coding, decoding and iterative decoding in Chapter 4. The standards of MB-OFDM UWB communications and UWB channels are given in Chapter 5. In Chapter 6, UWB cooperation methods are explained and error performance analysis is done in Chapter 7. Finally, experimental results and the conclusion are given in Chapter 8 and Chapter 9, respectively.

2. COOPERATIVE DIVERSITY

2.1. Diversity

To combat fading in wireless communications, we apply diversity techniques to improve the performance of the transmission. The diversity technique requires multiple replicas of the transmitted signals at the receiver, all carrying the same information but with small correlation in fading statistics. The idea is that if two or more independent samples of a signal are taken, these samples will fade in an uncorrelated manner, e.g., some samples are severely faded while others are less attenuated. The probability of all the samples being simultaneously below a given threshold is much lower than the probability of any individual sample being below that threshold [11].

Some well-known forms of diversity are time diversity, frequency diversity and spatial diversity. Time diversity can be achieved by transmitting identical messages in different time slots, which results in uncorrelated fading signals at the receiver. The required time separation is at least the coherence time of the channel. In mobile communications, error control coding is combined with interleaving to achieve time diversity. In this case, the replicas of the transmitted signals are usually provided to the receiver in the form of redundancy in the time domain introduced by error control coding. Since time interleaving results in decoding delays, this technique is usually effective for fast fading environments where the coherence time of the channel is small. One of the drawbacks of the scheme is that due to the redundancy introduced in the time domain, there is a loss in bandwidth efficiency.

To achieve frequency diversity, a number of different frequencies are used to transmit the same message. The frequencies need to be separated enough to ensure independent fading associated with each frequency. The uncorrelated fading statistics will be guaranteed by using frequency separation of the order of several times the channel coherence bandwidth. In mobile communications, the replicas of the transmitted signals are provided to the receiver in the form of redundancy in the frequency domain

introduced by spread spectrum such as direct sequence spread spectrum, multicarrier modulation and frequency hopping. Spread spectrum techniques are effective when the coherence bandwidth of the channel is small. Like time diversity, frequency diversity induces a loss in bandwidth efficiency due to a redundancy introduced in the frequency domain.

Space diversity is also called *antenna diversity*. It is typically implemented using multiple antennas or antenna arrays arranged together in space for transmission and/or reception as represented in Figure 2.1. The multiple antennas are separated physically by a proper distance so that the individual signals are uncorrelated. Typically a separation of a few wavelengths is enough to get uncorrelated signals. In space diversity, the replicas of the transmitted signals are usually provided to the receiver in the form of redundancy in the space domain. Unlike time and frequency diversity, space diversity does not induce any loss in bandwidth efficiency. This property is very attractive for future high data rate wireless communications such as 802.11n.

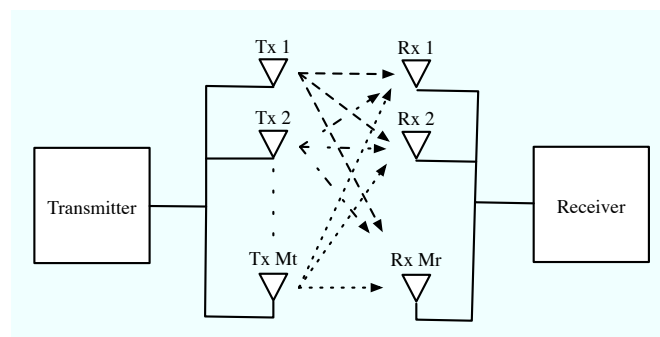


Figure 2.1. Space diversity with multiple transmit and receive antennas.

In general, the performance of communication systems with diversity techniques depends on how multiple signal replicas are combined at the receiver to increase the overall received signal-to-noise ratio (SNR). Therefore, diversity schemes can also be classified according to the type of combining methods employed at the receiver. According to the implementation complexity and the level of channel state information required by the combining method at the receiver, there are four main types of combining methods including selection combining, switched combining, equal-gain combining and maximal ratio combining.

In selection combining, which is a simple diversity combining method, the signal with the largest instantaneous SNR at every symbol interval is selected as the output, so that the output SNR is equal to that of the best incoming signal. In practice, the signal with the highest sum of the signal and noise power is usually used, since it is difficult to measure the SNR.

Switched combining diversity is obtained such that the receiver scans all the diversity branches and selects a particular one with the SNR above a certain threshold. This signal is selected as the output unless its SNR drops below the threshold. Then the receiver starts scanning again and switches to another branch. This method is inferior compared to selection diversity but it is simpler to implement as it does not require simultaneous and continuous observation of all the diversity branches. For both switched and selection combining schemes, only one of the branches is used as the output. In addition they do not require any channel state information, therefore, they can be used in conjunction with coherent and noncoherent modulations.

Maximal ratio combining is a linear combining method. In general, a linear combining process adds the weighted input signals together to get an output signal. The difference of methods depends on weighting factor selection. The output of combiner is given by

$$r = \sum_{i=1}^{M_r} \alpha_i r_i \quad (2.1)$$

where r_i is the signal received from i -th branch and α_i is the weighting coefficient of signal from branch i . In maximum ratio combining, the weighting factor of each receive antenna is chosen to be proportional to its own signal voltage to noise power ratio. Let A_i and θ_i be the amplitude and phase of the received signal r_i , respectively. Assuming that each antenna has the same average noise power, the weighting factor α_i can be represented as

$$\alpha_i = A_i e^{-j\theta_i}. \quad (2.2)$$

This method is called optimum combining since it can maximize the output SNR. In this scheme, each individual signal must be co-phased, weighted with its corresponding amplitude and then summed. This scheme requires the knowledge of channel fading amplitude and signal phases. So, it is not practical for noncoherent detection.

Equal gain combining is a suboptimal but simple linear combining method. The receiver sets the amplitudes of the weighting factors to be unity and they are used as

$$\alpha_i = e^{-j\theta_i}. \quad (2.3)$$

In this scheme, all the received signals are co-phased and added together with equal gain. The performance of equal-gain combining is only slightly inferior to maximum ratio combining and implementation complexity is significantly less than maximum ratio combining.

2.2. Cooperation

Applying spatial diversity with small mobile nodes is impractical because there is no place to put multiple antennas on a mobile node. So we need to introduce new techniques to implement spatial diversity on small devices. In general, mobile nodes are densely deployed and the distance between them is small. Also, the attenuation increases with the square of the distance. Thus, we can send data to nearer nodes with less power. We can use this fact to introduce diversity to our system. When we sent a signal to a destination, the neighbor nodes also receives that signal because the propagation of signals is circular. Since the neighbors are closer to sender than the destination, they can recover the data more accurately. Then, they can re-send it to destination and destination gets two different copies of same data. So, it can decode the data more correctly with the help of the information it obtain from second transmission. This scheme is known as user cooperation diversity. It is shown in [4] that we can obtain substantial gains over non-cooperative strategies.

Since the cooperation diversity techniques generally use the methods of relaying,

it is helpful to explain some of the relaying schemes. In general, these schemes are divided into three categories: repetition based protocols; coded cooperation diversity (CCD) and distributed turbo codes (DTC).

There are two simple repetition based protocols: decode-and-forward (DF) and amplify-and forward (AF). In DF, the relay decodes the source symbols and re-encodes them to send to destination. On the other hand, in AF, the relay does not decode the symbols. It simply amplifies and sends the symbols to destination. Both schemes use repetition codes, so no encoding is performed at the relay.

In other schemes (CCD and DTC), relay performs encoding. In CCD case, each node is matched to another node as a relay. The partner node acts as a relay only if it can correctly decode the source symbols. The relay decides to send by using cyclic redundancy check. This method requires the node to receive and send simultaneously. In addition, the synchronization between source and the relay must be accomplished to reduce the required bandwidth. In DTC case, the source transmits turbo encoded codewords. The relay receives the data, decodes it, interleaves the symbols and creates parity bits using a turbo encoder.

The performance analysis of some of the above methods can be found in [12], [13], [14] and [15]. They also propose some improvements on relaying techniques. The performance of such techniques under Ricean channels is analyzed in [16]. The impact of cooperative diversity on energy consumption and lifetime of sensor networks is analyzed in [17].

The full cooperation of transmission is achieved such that all cooperating nodes transmit both their own data and the neighbors' data. There are different mechanisms to implement cooperation in wireless networks. One of the well known cooperation models is proposed in [4]. In that model, each user sends both its own data and its partner's data, as it is shown in Figure 2.2. In the figure, X 's are transmitted signals, Y 's are received signals, Z 's are noise components and K 's are fading coefficients. The model assumes that echo cancellation is possible at the mobiles. The transmitted sig-

nals have an average power constraint, the noise terms are zero-mean complex Gaussian random processes and the fading coefficients are zero-mean complex Gaussian random variables. It is also assumed that the base station (BS) and the mobiles can track fading coefficients, in other words, all the decoding is done with the knowledge of fading parameters. The system is assumed to be synchronous for simplicity of analysis.

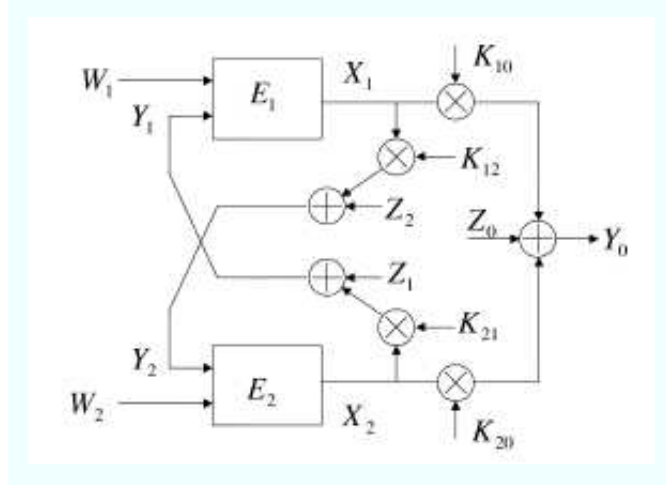


Figure 2.2. Cooperation model of Sendonaris *et al.*

A CDMA implementation is also given in [4] and its aspects are studied in [5]. Each user modulates one bit on to its spreading code. The users' codes are orthogonal and the coherence time of the channel is \$L\$ symbol periods. Without cooperation, each user sends a new data bit at each symbol period. In cooperative case, the periods are used such that, in first period users only send data to BS. In the second period, mobiles send data to both BS and the partner mobile. The signals for each period are:

$$X_1(t) = a_{11}b_1^1c_1(t), \quad a_{12}b_1^2c_1(t), \quad a_{13}b_1^2c_1(t) + a_{14}\hat{b}_2^2c_2(t) \quad (2.4)$$

$$X_2(t) = \underbrace{a_{21}b_2^1c_2(t)}_{\text{Period 1}}, \quad \underbrace{a_{22}b_2^2c_2(t)}_{\text{Period 2}}, \quad \underbrace{a_{23}\hat{b}_1^2c_1(t) + a_{24}b_2^2c_2(t)}_{\text{Period 3}} \quad (2.5)$$

In that case, only 2 bits per 3 symbol periods are sent instead of 3 bits, but it is shown in [4] and [5] that the throughput is increased. Another possibility is for the two users to always send new information, even during the cooperative periods. However, that situation necessitates the use of sequence detection due to the intersymbol interference.

In general, the cooperation is performed via eavesdropping of the data sent by a cooperating user and re-transmission of it. Those schemes are only capable of second-order diversity. Multiple Source Cooperation (MSC) diversity, which is proposed in [18] consists joint encoding of data from multiple users by one or more cooperating users. It is assumed that the channels between users are flat, slowly varying fading process which are known to the users and statistically independent from each other. There is also AWGN which is effective on outputs of channels. There are N users transmitting to a single destination in a TDMA network. The model can be applied to other types of networks such as FDMA and CDMA. In MSC, first, the users transmit their data to both destination and other users in network. Each user listens to the transmissions of other users. After that, one or more cooperating users apply error correction code (ECC) encoders to the data they received from neighbor users and transmits the parity data to the destination. Destination uses that parity data to recover channel fading events.

When the user-to-user channel is not good enough, the parity data becomes false. We can overcome that by refraining from parity data which come from bad channel's user. It is shown in [18] that MSC can achieve a diversity order of D with a code rate of $1 - (D - 1)/N$, where $0 < D \leq N$ and N is the number of cooperating users. When there are more users to cooperate, we obtain higher diversity gains and code rates.

Another most studied scenario is the STC cooperation. Since it is not feasible to use space time block codes (STBC) in communication where the mobile users such as sensor nodes cannot carry multiple antennas, cooperative STBC schemes are used. Cooperative STBC not only increase transmission energy efficiency, but also distribute energy consumption evenly over multiple sensors. But there are issues to examine such that the associated overhead, synchronization, and energy efficiency. For that purpose, a typical networking/communication protocol, i.e. low-energy adaptive clustering hierarchy (LEACH) is introduced in [3]. The system model consists of a wireless sensor network where sensors need to transmit data to a remote collector. In LEACH, the sensors form hierarchical clusters and schedule TDMA channel access. The LEACH operates in rounds which is divided into 4 different phases: advertisement, cluster

setup, transmission scheduling and data transmission.

In advertisement phase, each node determines whether it becomes a cluster head or not during current round. The cluster heads broadcast an advertisement message to neighbor nodes. Cluster heads are named *primary head*. In cluster setup, each setup decides its primary head and transmits a cluster-joining packet to it. That packet also includes information about the node's current energy status, etc. For a J -sensor cooperation, we need to choose $J - 1$ *secondary heads* among all transmitting nodes. The choice of secondary heads is performed in the next phase. In scheduling phase, each primary head decides on TDMA channel access schedule and selects secondary heads based on their reported energy status and received signal power. The secondary head selection details are explained in [3]. The selection decision is sent to secondary nodes with a 1 bit overhead in the original scheduling packet. In data transmission phase, if there is not any cooperation, the cluster head receives data packets from other sensors and sends them to data collector. When there is cooperative transmission, the cluster head first sends data packets to secondary heads, and all the J nodes transmit data cooperatively to the data collector. [3] assumes that the transmission is perfectly synchronous. The imperfect synchronization case is analyzed in [19]. The model is illustrated in Figure 2.3.

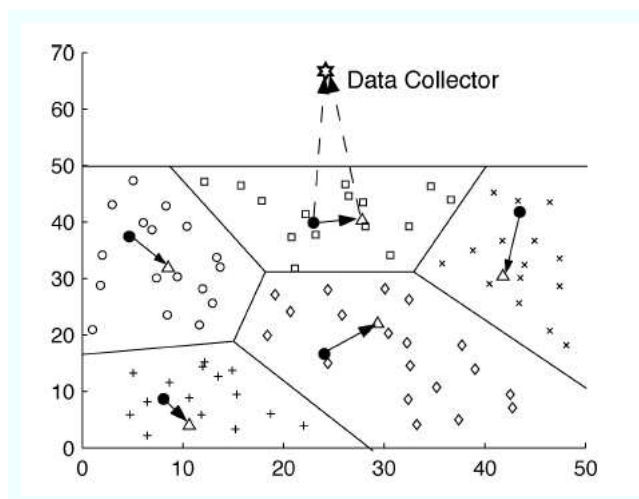


Figure 2.3. Cooperative transmission model of LEACH [3]. \bullet : primary heads, \triangle : secondary heads.

The first phase does not introduce any overhead depending on cooperative trans-

mission because this phase is same in ordinary LEACH model. The second phase's overhead will be one extra byte added to the cluster joining packet, which is relatively long. The third phase introduces 1 bit overhead as explained above. The most important overhead comes from the last phase. In last phase, the data packets are broadcasted to secondary heads, and there are also an overhead depending on electronic energy consumption. According to above facts, LEACH is a good model to implement cooperative transmission with small overhead.

In [3] it is also shown that, cooperative transmission in LEACH is efficient if the distance between the data collector and the cluster is bigger than a threshold. That threshold depends on both STBC scheme and the number of cooperative nodes.

Another scheme with STBC is studied by Laneman in [2]. They developed and analyzed space-time coded cooperative diversity protocols in which the nodes that correctly decode the source's signal joins the cooperation.

3. SPACE-TIME CODING

Coding techniques designed for multiple antenna transmission to achieve space and time diversity are called space-time coding (STC). STCs rely on transmitting multiple, redundant copies of a data stream to the receiver in the hope that at least some of them may survive the physical path between transmission and reception in a good enough state to allow reliable decoding. In particular, coding is performed by adding properly designed redundancy in both spatial and temporal domains, which introduces correlation into the transmitted signals. Due to joint design, space-time codes can achieve transmit diversity as well as a coding gain without sacrificing bandwidth.

The STC system is composed of M_t transmit and M_r receive antennas as shown in Figure 2.1. The overall channel is made up of $M_t \times M_r$ slowly varying sub-channels. At any time interval, M_t signals are transmitted simultaneously, one from each transmit antenna. The sub-channels undergo independent fading. The fade coefficients are assumed to be fixed during a slot and independent from slot to another. The transmitted code vector and channel matrix at time t can be written as

$$c_t = [c_1(t), c_2(t), \dots, c_{M_t}(t)]^T \quad (3.1)$$

$$H_t = \begin{bmatrix} h_{1,1}^t & h_{1,2}^t & \cdots & h_{1,M_t}^t \\ h_{2,1}^t & h_{2,2}^t & \cdots & h_{2,M_t}^t \\ \vdots & \vdots & \ddots & \vdots \\ h_{M_r,1}^t & h_{M_r,2}^t & \cdots & h_{M_r,M_t}^t \end{bmatrix}. \quad (3.2)$$

The received signal is

$$r_t = H_t c_t + n_t \quad (3.3)$$

where n_t denotes noise vector. We define a transmitted vector sequence of length- L which gives the space-time codeword matrix such that

$$C = [c_1, c_2, \dots, c_L] \quad (3.4)$$

At each time instant, one column of C is transmitted from M_t antennas simultaneously. The choice of codeword symbols defines the type of STC. The decoder at the receiver uses a maximum likelihood algorithm to estimate the transmitted information sequence. The decision metric is computed based on the squared Euclidian distance between the hypothesized received sequence and the actual sequence as

$$\sum_t \sum_{j=1}^{M_r} \left| r_j(t) - \sum_{i=1}^{M_t} h_{j,i}^t c_i(t) \right|^2. \quad (3.5)$$

The decoder selects a codeword with the minimum decision metric as the decoded sequence.

Two types of STC are developed; Trellis Codes and Block Codes. Since the decoding complexity of trellis codes increases exponentially as a function of the diversity level and transmission rate [20], we preferred block codes because they can be decoded using simple linear processing at the receiver under the assumption of flat fading Rayleigh channels.

There have been many approaches to STBCs, the scheme of Alamouti being the first [1]. The key feature is that it achieves a full diversity gain with a simple maximum likelihood decoding algorithm. The code matrix Alamouti proposed is

$$c = \begin{bmatrix} s_0 & -s_1^* \\ s_1 & s_0^* \end{bmatrix} \quad (3.6)$$

where s_0 and s_1 are information symbols. It is clear that the encoding is done in both the space and time domains. Assuming channel is quasi-static such that it is constant

during two time slots, the received signals in two time slots can be denoted as

$$\begin{aligned} r_0 &= h_0 s_0 + h_1 s_1 + n_0 \\ r_1 &= -h_0 s_1^* + h_1 s_0^* + n_1. \end{aligned} \quad (3.7)$$

where $h_0 = \alpha_0 e^{j\theta_0}$ and $h_1 = \alpha_1 e^{j\theta_1}$ are flat fading constants of the channel, n_0 and n_1 are additive white Gaussian noise samples at two time slots. We can combine them by

$$\begin{aligned} \tilde{s}_0 &= h_0^* r_0 + h_1 r_1^* \\ \tilde{s}_1 &= h_1^* r_0 - h_0 r_1^* \end{aligned} \quad (3.8)$$

and send to maximum likelihood decoder as

$$\begin{aligned} \tilde{s}_0 &= (\alpha_0^2 + \alpha_1^2) s_0 + h_0^* n_0 + h_1 n_1^* \\ \tilde{s}_1 &= (\alpha_0^2 + \alpha_1^2) s_1 - h_0 n_1^* + h_1^* n_0. \end{aligned} \quad (3.9)$$

Thus, the maximum likelihood decoding rule chooses the symbol closest to \tilde{s}_i such that

$$\begin{aligned} \hat{s}_0 &= \arg \min_{\hat{s}_0 \in \mathcal{S}} d^2(\tilde{s}_0, \hat{s}_0) \\ \hat{s}_1 &= \arg \min_{\hat{s}_1 \in \mathcal{S}} d^2(\tilde{s}_1, \hat{s}_1). \end{aligned} \quad (3.10)$$

where $d^2(\cdot)$ is the squared Euclidian distance between two M-PSK symbols.

Alamouti code can be applied with two transmit and M_r receive antennas. The received signals at j -th antenna in two time slots becomes

$$\begin{aligned} r_0^j &= h_{j,0} s_0 + h_{j,1} s_1 + n_0^j \\ r_1^j &= -h_{j,0} s_1^* + h_{j,1} s_0^* + n_1^j \end{aligned} \quad (3.11)$$

where $h_{j,i}$, $i = 0, 1, j = 1, \dots, M_r$ is the fading coefficient for the path from transmit antenna i to receive antenna j . The receiver constructs two decision statistics such

that

$$\begin{aligned}\tilde{s}_0 &= \sum_{j=1}^{M_r} h_{j,0}^* r_0^j + h_{j,1} (r_1^j)^* \\ \tilde{s}_1 &= \sum_{j=1}^{M_r} h_{j,1}^* r_0^j - h_{j,0} (r_1^j)^*.\end{aligned}\quad (3.12)$$

The decoding rule is the same with single receive antenna case. The performance of Alamouti code and comparison with MRC can be seen in Figure 3.1.

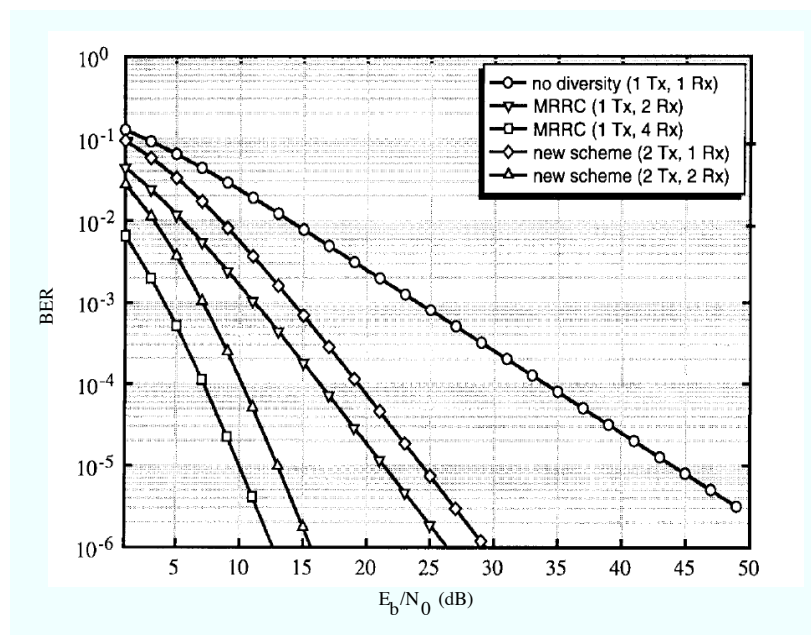


Figure 3.1. The BER performance comparison of coherent BPSK with maximal ratio receiver combining (MRRC) and two-branch transmit diversity in Rayleigh fading [1].

The Alamouti scheme achieves the full diversity with a very simple maximum likelihood decoding algorithm. The key feature of the scheme is orthogonality between sequences generated by the two antennas. This scheme was generalized to an arbitrary number of transmit antennas by applying the theory of orthogonal designs [21]. In general, a space-time block code is defined by an $M_t \times p$ transmission matrix X . M_t represents the number of antennas and p represents the number of time periods for transmission of one block of coded symbols.

Let us assume that the signal constellation consists of 2^m points. At each encoding operation, a block of km information bits are mapped into the signal constellation to

select k modulated signals x_1, x_2, \dots, x_k . The k modulated signals are encoded by a space-time block encoder to generate M_t parallel signal sequences of length p according to the transmission matrix X . These sequences are transmitted through M_t antennas simultaneously in p time periods.

The *rate* of a space-time block code is defined as the ratio between the number of symbols the encoder takes as its input and the number of space-time coded symbols transmitted from each antenna. It is given by

$$R = k/p. \quad (3.13)$$

The spectral efficiency of the space-time block code is calculated as

$$\eta = \frac{r_b}{B} = \frac{r_s m R}{r_s} = \frac{km}{p} \text{bits/s/Hz} \quad (3.14)$$

where r_b and r_s are the bit and symbol rate, respectively, and B is the bandwidth.

The entries of the transmission matrix X are linear combinations of the k modulated symbols x_1, x_2, \dots, x_k and their conjugates $x_1^*, x_2^*, \dots, x_k^*$. In order to achieve the full transmit diversity of M_t , the transmission matrix X is constructed based on orthogonal designs such that [21]

$$X \bullet X^H = c(|x_1|^2 + |x_2|^2 + \dots + |x_k|^2)I_{M_t} \quad (3.15)$$

where c is a constant, X^H is the Hermitian of X and I_{M_t} is an $M_t \times M_t$ identity matrix. The i th row of X represents the symbols transmitted from i th transmit antenna consecutively in p transmission periods, while the j th column of X represents the symbols transmitted simultaneously through M_t antennas at time j .

The orthogonality enables to achieve the full transmit diversity for a given number of transmit antennas. In addition, it allows the receiver to decouple the signals transmitted from different antennas and consequently, a simple maximum likelihood

decoding, based only on linear processing of the received signals.

The Alamouti scheme is unique in that it is the only space-time block code with an $M_t \times M_t$ complex transmission matrix to achieve the full rate [21]. If the number of the transmit antennas is larger than two, the code design goal is to construct high-rate complex transmission matrices with low decoding complexity that achieve the full diversity. In addition, the value of p must be minimized in order to minimize the decoding delay.

For an arbitrary complex signal constellation, there are space-time block codes that can achieve a rate of 1/2 for any given number of antennas. For example, complex transmission matrices X_3^c and X_4^c [21] are orthogonal designs for space-time block codes with three and four antennas, respectively. These codes have the rate 1/2.

$$X_3^c = \begin{bmatrix} x_1 & -x_2 & -x_3 & -x_4 & x_1^* & -x_2^* & -x_3^* & -x_4^* \\ x_2 & x_1 & x_4 & -x_3 & x_2^* & x_1^* & x_4^* & -x_3^* \\ x_3 & -x_4 & x_1 & x_2 & x_3^* & -x_4^* & x_1^* & x_2^* \end{bmatrix} \quad (3.16)$$

$$X_4^c = \begin{bmatrix} x_1 & -x_2 & -x_3 & -x_4 & x_1^* & -x_2^* & -x_3^* & -x_4^* \\ x_2 & x_1 & x_4 & -x_3 & x_2^* & x_1^* & x_4^* & -x_3^* \\ x_3 & -x_4 & x_1 & x_2 & x_3^* & -x_4^* & x_1^* & x_2^* \\ x_4 & x_3 & -x_2 & x_1 & x_4^* & x_3^* & -x_2^* & x_1^* \end{bmatrix} \quad (3.17)$$

A more involved linear processing results in a higher rate for space-time block codes with a complex constellation and more than two antennas. The following two matrices X_3^h and X_4^h are complex generalized orthogonal designs for space-time block

codes with rate 3/4 [21].

$$X_3^h = \begin{bmatrix} x_1 & -x_2^* & \frac{x_3^*}{\sqrt{2}} & \frac{x_3^*}{\sqrt{2}} \\ x_2 & x_1^* & \frac{x_3^*}{\sqrt{2}} & \frac{-x_3^*}{\sqrt{2}} \\ \frac{x_3}{\sqrt{2}} & \frac{x_3}{\sqrt{2}} & \frac{-x_1-x_1^*+x_2-x_2^*}{2} & \frac{x_2+x_2^*+x_1-x_1^*}{2} \end{bmatrix} \quad (3.18)$$

$$X_4^h = \begin{bmatrix} x_1 & -x_2^* & \frac{x_3^*}{\sqrt{2}} & \frac{x_3^*}{\sqrt{2}} \\ x_2 & x_1^* & \frac{x_3^*}{\sqrt{2}} & \frac{-x_3^*}{\sqrt{2}} \\ \frac{x_3}{\sqrt{2}} & \frac{x_3}{\sqrt{2}} & \frac{-x_1-x_1^*+x_2-x_2^*}{2} & \frac{x_2+x_2^*+x_1-x_1^*}{2} \\ \frac{x_3}{\sqrt{2}} & \frac{-x_3}{\sqrt{2}} & \frac{-x_2-x_2^*+x_1-x_1^*}{2} & \frac{-(x_1+x_1^*+x_2-x_2^*)}{2} \end{bmatrix} \quad (3.19)$$

Another rate 3/4 space-time block code with three antennas over complex constellations shown in [11] is given by

$$X_3^{h'} = \begin{bmatrix} x_1 & x_2^* & x^* & 0 \\ -x_2 & x_1^* & 0 & -x_3^* \\ -x_3 & 0 & x_1^* & x_2^* \end{bmatrix} \quad (3.20)$$

The decoding of STBC involves linear processing as explained before. For the rate 1/2 STBC X_3^c and X_4^c , the decision statistics \tilde{x}_i can be represented by

$$\tilde{x}_i = \sum_{t \in \eta(i)} \sum_{j=1}^{M_r} \text{sgn}_t(i) \cdot \tilde{r}_t^j(i) \cdot \tilde{h}_{j, \epsilon_t(i)} \quad (3.21)$$

where ϵ_t denote the permutations of the symbols from the first column to the t-th column,

$$\tilde{r}_t^j(i) = \begin{cases} r_t^j & \text{if } x_i \text{ belongs to the t-th column of } X_{M_t}^c \\ (r_t^j)^* & \text{if } x_i^* \text{ belongs to the t-th column of } X_{M_t}^c \end{cases} \quad (3.22)$$

and

$$\tilde{h}_{j,\epsilon t(i)} = \begin{cases} h_{j,\epsilon t(i)}^* & \text{if } x_i \text{ belongs to the } t\text{-th column of } X_{M_t}^c \\ h_{j,\epsilon t(i)} & \text{if } x_i^* \text{ belongs to the } t\text{-th column of } X_{M_t}^c \end{cases}. \quad (3.23)$$

The simulation results in Figure 3.2 represents the performance of STBC on Rayleigh fading channels. It is assumed that the receiver knows the perfect channel state information. The performance is shown for two, three and four antenna transmission and single antenna reception. The STBC with two transmit antennas is the rate one code X_2^c with QPSK modulation. The STBC with three and four transmit antennas are the rate 1/2 codes X_3^c and X_4^c , respectively, with 16-QAM modulation.

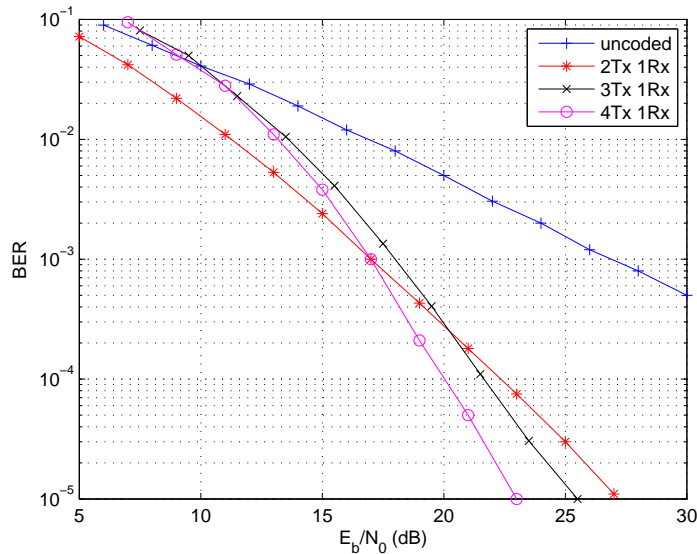


Figure 3.2. The BER performance comparison of space-time coded communications at 2bits/s/Hz rate with different number of transmit antennas and one receive antenna.

Under frequency selective channel conditions, we need to apply different techniques to combat inter-symbol interference (ISI). One of those methods is using equalization. Equalization is passing the received signal through a filter which is inverse of the channel to cancel the effect of it. Another method is using OFDM which is dividing the channel into frequency-flat fading sub-channels.

In [22], they propose some time domain and frequency domain equalization techniques for STBC. In [23], they implement their STBC equalization techniques to cooperative signaling. They assume S-R-D path as one channel and S-D path as another channel. They use three different techniques which are Distributed Single Carrier STBC, Distributed Time Reversal STBC, and Distributed STBC-OFDM. In their cooperation architecture, first the Source sends its data to Relay, then, they transmit cooperatively to Destination. They investigate distributed STBC-OFDM in [24] and Distributed Time Reversal STBC in [25] in details.

In [26] OFDM with coded cooperation is proposed. The time slot of a user is divided into two sub-slots and the data of a user is divided into transmissions of both users. At first slot, user sends half of its codewords with OFDM. If user 2 correctly decodes the signal, it sends the second half of codewords to destination. If not, user 1 transmits the second half of codewords itself. The symbols at each sub-carrier can be processed separately.

In [27], they propose a three time slot length cooperation using amplify-and-forward method with OFDM transmission. Each user has a subcarrier set which is disjoint from other users' sets. They use both inter-block and intra-block precoding to exploit temporal and multipath diversity, respectively.

To deal with severe frequency-selectivity of UWB channels, we employed MB-OFDM, which is simple but powerful method such that we only need one-tap equalization at each sub-channel and use IFFT-FFT pair for modulation and demodulation.

4. CONVOLUTIONAL CODING AND MAP DECODING

The main goal of a digital communication system is transmitting information from one end of the system to a user at the other end at a rate which ensures a level of reliability and quality that are acceptable [28]. The aim of error control coding is improving channel capacity, which defines the maximum data rate of the channel for a given level of reliability, changing data quality from problematic to acceptable and reduce the required E_b/N_0 for a fixed bit error rate.

The two basic types of encoding is block coding and convolutional coding. In block coding, the input stream is divided into segments with a fixed length and these segments are processed in blocks to give output segments of fixed length. In other words, there is a fixed length codeword for each input segment. In convolutional codes which were first introduced by Elias in 1955 as an alternative to block codes the encoder system has memory, thus the output is affected by every input bits [29]. The whole output is a codeword.

Our choice is convolutional codes which are constructed by the usage of linear shift registers. The outputs of a convolutional encoder is obtained by modulo-2 addition of the outputs of memory elements with different permutations. The permutations are stored in a generator matrix, g , which can be obtained as the output of encoder when input is unit impulse (a 1 bit and a lot of 0s). The modulo 2 convolution of input and state of memory elements with generator matrix gives the output.

One of the properties of a convolutional encoder is its rate R which is given by k/n where k and n are the number of inputs and outputs of the encoder. There are n outputs for k input bits. Another one is the constraint length K which is the number of output bits affected by one bit. K is defined as

$$K \triangleq 1 + \max_i m_i$$

where m_i is the length of longest shift register.

The convolutional codes can be divided into two groups such as systematic and non-systematic codes. Systematic codes include the input as a block at the output, non-systematic codes don't. Another classification is feedforward and feedback encoders. An example for a rate 1/2 binary nonsystematic feedforward convolutional encoder is given in Figure 4.1.

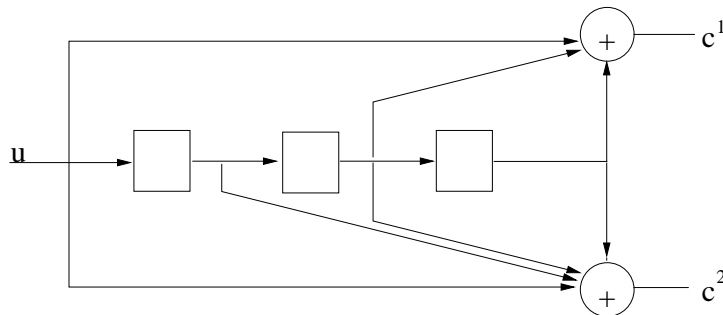


Figure 4.1. Rate 1/2 binary nonsystematic feedforward convolutional encoder with memory order $m=3$.

The boxes are memory units. The generator polynomials for Figure 4.1 are

$$g^1 = (1011) \quad (4.1)$$

$$g^2 = (1011). \quad (4.2)$$

The outputs c^1 and c^2 are calculated by modulo-2 convolution.

$$c_l^1 = \sum_{i=0}^3 u_{l-i} g_i^1 \quad (4.3)$$

$$c_l^2 = \sum_{i=0}^3 u_{l-i} g_i^2. \quad (4.4)$$

To show the relation between input/output and state of memory elements, we can construct a diagram, such as in Figure 4.2, called “trellis diagram”. This diagram shows state of shift registers before and after a transition. Transitions are labelled with corresponding input bit and the output bits.

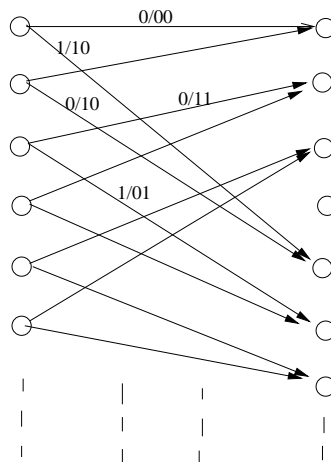


Figure 4.2. A sample trellis diagram with 1 input and 2 output bits.

4.1. Decoding of Convolutional Codes

In 1961 Wozencraft and Reiffen introduced “sequential decoding” as an efficient decoding algorithm for convolutional codes [30]. It was a suboptimal decoding algorithm. In 1963, Massey proposed “threshold decoding”, which is simpler-to-implement but less efficient [31]. In 1967, Viterbi presented a maximum likelihood decoding algorithm which is asymptotically optimum [32]. This algorithm was relatively easy to implement for soft-decision decoding of convolutional codes. In 1974, Bahl, Cocke, Jelinek, and Raviv (BCJR) presented a maximum a posteriori probability (MAP) decoding algorithm for the information bits [33]. In recent years, this algorithm has been adapted to soft-decision iterative decoding schemes. We will present MAP algorithm only.

4.1.1. MAP Algorithm for Rate 1/n Convolutional Codes with AWGN Channel

In MAP algorithm, the inputs of decoder are the received sequence \mathbf{r} and the a priori log-likelihood values of the information bits. The algorithm calculates a posteriori L-values as

$$L(u_l) = \ln \frac{P(u_l = +1|\mathbf{r})}{P(u_l = -1|\mathbf{r})}. \quad (4.5)$$

The probabilities inside the logarithm can be written as

$$\begin{aligned} \frac{P(u_l = +1|\mathbf{r})}{P(u_l = -1|\mathbf{r})} &= \frac{P(u_l = +1, \mathbf{r})}{P(u_l = -1, \mathbf{r})} \\ &= \frac{\sum_{(s',s) \in \Sigma_l^+} p(s_l = s', s_{l+1} = s, \mathbf{r})}{\sum_{(s',s) \in \Sigma_l^-} p(s_l = s', s_{l+1} = s, \mathbf{r})} \end{aligned} \quad (4.6)$$

by using the trellis. Σ_l^+ denotes the transitions between states s' and s when input bit is +1. The probabilities $p(s_l = s', s_{l+1} = s, \mathbf{r})$ can be divided into three partitions which are

$$p(s_l, s_{l+1}, \mathbf{r}) = \alpha_l(s') \gamma_l(s', s) \beta_{l+1}(s) \quad (4.7)$$

$$\alpha_l(s') \equiv p(s', \mathbf{r}_{t < l}) \quad (4.8)$$

$$\beta_{l+1}(s) \equiv p(\mathbf{r}_{t > l} | s) \quad (4.9)$$

$$\gamma_l(s', s) \equiv p(s, \mathbf{r}_l | s'). \quad (4.10)$$

The α and β can be calculated by a recursion which employs γ . The recursions are obtained by writing the probability $p(s, \mathbf{r}_{t < l+1})$ as a summation of $p(s, s', \mathbf{r}_{t < l+1})$ over s' and dividing $p(s, s', \mathbf{r}_{t < l+1})$ into 2 parts. Finally we have

$$\alpha_{l+1}(s) = \sum_{s' \in \sigma_l} \gamma_l(s', s) \alpha_l(s') \quad (4.11)$$

$$\beta_l(s) = \sum_{s \in \sigma_{l+1}} \gamma_l(s', s) \beta_{l+1}(s'). \quad (4.12)$$

To start the recursions, we need initial conditions. Since the encoder starts in all-zero state, $\alpha_0(0) = 1$ and $\alpha_0(s \neq 0) = 1$. Same situation holds for β too because the encoder ends in all-zero state.

The branch metric, $\gamma_l(s', s)$ for a AWGN channel can be calculated by Gaussian

probability density function as

$$\begin{aligned}
\gamma_l(s', s) &= p(s, \mathbf{r}_l | s') \\
&= P(u_l) p(\mathbf{r}_l | \mathbf{c}_l) \\
&= P(u_l) \left(\frac{1}{\sqrt{2\pi\sigma^2}} \right)^n e^{-\frac{\|\mathbf{r}_l - \mathbf{c}_l\|^2}{2\sigma^2}}
\end{aligned} \tag{4.13}$$

where n is the number of output bits for 1 input bit.

The $(\frac{1}{\sqrt{2\pi\sigma^2}})^n$ is a factor of every element of both numerator and denominator of Equation 4.6 so we can eliminate it.

If we use logarithms of α , β and γ 's, we obtain

$$\gamma_l^*(s', s) = \ln P(u_l) + \ln \left(\frac{1}{\sqrt{2\pi\sigma^2}} \right)^n - \frac{\|\mathbf{r}_l - \mathbf{c}_l\|^2}{2\sigma^2}. \tag{4.14}$$

In addition, suppose $n = 1$. Adding a constant to $\ln P(r_l | c_l)$ to make all γ 's multiplied by a constant which will result in no modification at all in the main log-likelihood equation due to the fact that constant will appear in both the numerator and the denominator. Now, replace $\log P(r_l | c_l)$ by,

$$\ln P(r_l | c_l) - \frac{1}{2} \ln P(r_l | c_l = 1) - \frac{1}{2} \ln P(r_l | c_l = -1). \tag{4.15}$$

It can be observed that this expression will have the values of $\frac{1}{2} \log \frac{P(r_l | c_l = 1)}{P(r_l | c_l = -1)}$ and $\frac{1}{2} \log \frac{P(r_l | c_l = -1)}{P(r_l | c_l = 1)}$ when $c_k = 1$ and $c_k = -1$ respectively. So our new expression for

$\log P(r_l | c_l)$ is,

$$\begin{aligned}
\log P(r_l | c_l) &= \frac{1}{2} c_l \ln \frac{P(r_l | c_l = 1)}{P(r_l | c_l = -1)} \\
&= \frac{1}{2} c_l \left[-\frac{1}{2\sigma^2} ((r_l - 1)^2 - (r_l + 1)^2) \right] \\
&= \frac{1}{2} \frac{1}{2\sigma^2} 4c_l r_l = \frac{1}{2} \left(\frac{2}{\sigma^2} \right) r_l c_l \\
&= \frac{1}{2} L_c r_l c_l
\end{aligned} \tag{4.16}$$

If $n > 1$ the expression becomes

$$\ln P(r_l | c_l) = \frac{1}{2} L_c \sum_{i=1}^n r_l^i c_l^i \tag{4.17}$$

If we apply the same procedure to $P(u_l)$, we obtain

$$\gamma_l^*(s', s) = \frac{1}{2} L_c \sum_{i=1}^n r_l^i c_l^i + \frac{1}{2} u_l L_a(u_l). \tag{4.18}$$

The final LLR becomes

$$\frac{P(u_l = +1 | \mathbf{r})}{P(u_l = -1 | \mathbf{r})} = \frac{\sum_{(s', s) \in \Sigma_l^+} e^{\alpha_l^*(s') + \gamma_l^*(s', s) + \beta_{l+1}^*(s)}}{\sum_{(s', s) \in \Sigma_l^-} e^{\alpha_l^*(s') + \gamma_l^*(s', s) + \beta_{l+1}^*(s)}}. \tag{4.19}$$

By applying same modifications, we obtain LLR's for code bits as

$$L(c_l) = \ln \frac{\sum_{(s', s) \in \Sigma_l^+} e^{\alpha_l^*(s') + \gamma_l^*(s', s) + \beta_{l+1}^*(s)}}{\sum_{(s', s) \in \Sigma_l^-} e^{\alpha_l^*(s') + \gamma_l^*(s', s) + \beta_{l+1}^*(s)}} \tag{4.20}$$

where Σ_l^+ denotes the transitions in which the code bit is +1.

4.2. Iterative Decoding

It is shown in [34] that we can obtain substantial gains by employing iterative decoding. The system employs soft demodulator which calculates log-likelihood ratios (LLR) of code bits from received symbols and *a priori* LLR values fed back from a log-MAP decoder which uses the information from soft demodulator.

The iterative decoding scheme is presented in Figure 4.3. c' is the output convolutionally encoding the information bits u . After interleaver, which increases redundancy against burst noise, the bits are modulated to symbols s to transmit over channel. At the receiver, the received signal y is processed by a soft demapper, which outputs LLRs $L(c)$. These LLRs are combined with *a priori* LLRs $L_a(c)$ from the LogMAP decoder to produce extrinsic LLRs $L_e(c)$. The extrinsic LLRs are then passed through an interleaver to produce *a priori* LLRs $L_a(c')$ for the next iteration.

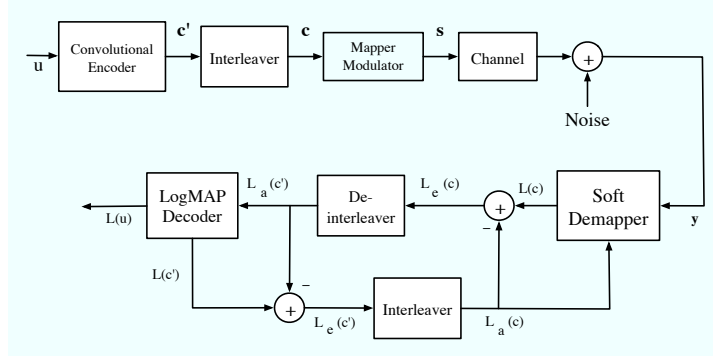


Figure 4.3. Iterative decoding system.

At the receiver, soft demapper assumes $L_a(c)$ as zero at first iteration when calculating output *a posteriori* LLRs $L(c)$ such that

$$\begin{aligned}
 L(c_{k,l}) &= \log \frac{P(c_{k,l} = 1 | Y_k)}{P(c_{k,l} = -1 | Y_k)} = \log \frac{\sum_{\forall S_k: c_{k,l}=1} \exp(K(S_k)) \prod_{m=1}^2 P(c_{k,m})}{\sum_{\forall S_k: c_{k,l}=-1} \exp(K(S_k)) \prod_{m=1}^2 P(c_{k,m})} \\
 &= \underbrace{\log \frac{P(c_{k,l} = 1)}{P(c_{k,l} = -1)}}_{L_a(c_{k,l})} + \underbrace{\log \frac{\sum_{\forall S_k: c_{k,l}=1, l \neq m} \exp(K(S_k) + \frac{1}{2} c_{k,m} L_a(c_{k,m}))}{\sum_{\forall S_k: c_{k,l}=1, l \neq m} \exp(K(S_k) + \frac{1}{2} c_{k,m} L_a(c_{k,m}))}}_{L_e(c_{k,l})} \quad (4.21)
 \end{aligned}$$

where

$$K(S_k) = -\frac{1}{2\sigma^2} |Y_k - \Lambda S_k|^2,$$

$L_a(c_{k,l})$ and $L_e(c_{k,l})$ are *a priori* and extrinsic LLRs of bit $c_{k,l}$ (see Appendix A for

derivation). In order to reduce the computational complexity and to avoid numerical instability, The extrinsic LLR $L_e(c_{k,l})$ can be calculated by

$$L_e(c_{k,l}) = \max_{\forall S_k: c_{k,l}=1, l \neq m}^* \left[K(S_k) + \frac{1}{2} c_{k,m} L_a(c_{k,m}) \right] - \max_{\forall S_k: c_{k,l}=-1, l \neq m}^* \left[K(S_k) + \frac{1}{2} c_{k,m} L_a(c_{k,m}) \right] \quad (4.22)$$

where $\max^*[\cdot, \cdot]$ operation is defined as $\max^*[x, y] = \max[x, y] + \log(1 + e^{-|x-y|})$.

Then $L_a(c)$ is subtracted from the output of soft demapper to feed extrinsic information to deinterleaver. The log-MAP decoder which is explained in Section 4.1 is used to calculate $L(u)$ and $L(c')$, LLRs of information bits and codebits, respectively. For iterative decoding, $L(c')$ is fed back to soft demapper after passing it through interleaver again.

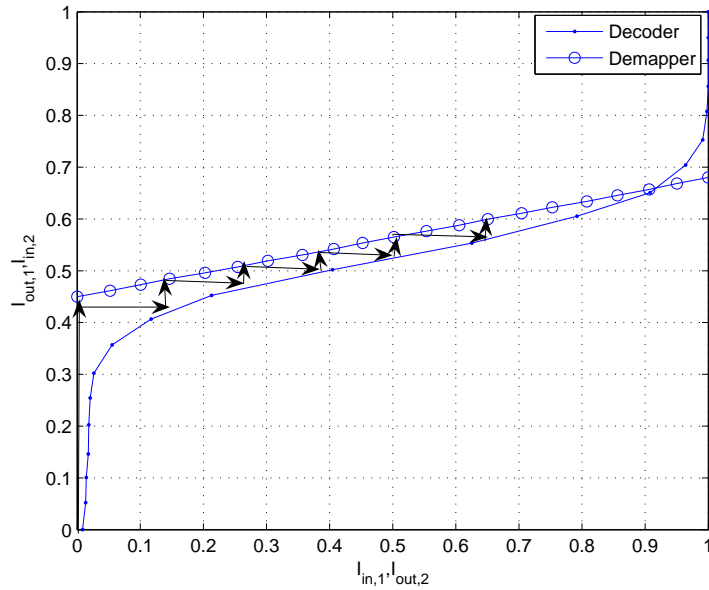


Figure 4.4. Example EXIT chart for iterative decoding system.

We can measure the performance gain of iterative receiver by Extrinsic Information Transfer (EXIT) charts as shown in Figure 4.4. $I_{in,1}$ and $I_{out,1}$ are input and output mutual information of codebits at soft demapper respectively. $I_{in,2}$, $I_{out,2}$ are input and output mutual information of log-MAP decoder respectively. The calculation of those mutual information employs probability distributions of LLR values of bits as defined

in [34].

From Figure 4.4, we can see the improvement of mutual information of codebits through iterations. At first iteration, the input information of soft demapper is zero. Soft demapper calculates its output LLRs only from channel observations. Then, the output information of demapper is fed to log-MAP decoder whose input is on vertical axis as output of demapper. Then, the output of decoder is fed back to demapper and after some number of iterations, we get a performance improvement as the BER graph in Figure 4.5 shows.

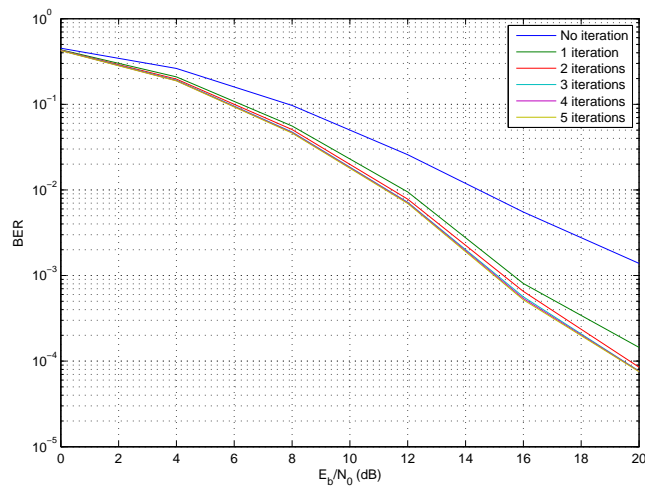


Figure 4.5. Iterative decoding performance of MB OFDM system.

5. MULTIBAND OFDM ULTRA WIDEBAND SYSTEM

In our study, we consider the MB-OFDM UWB system which is represented in Figure 5.1. Basically, the symbol sequence is passed through inverse fast Fourier transform (IFFT) and time domain signal is transmitted to receiver after digital-analog conversion. In MB-OFDM, the bandwidth of an OFDM symbol is 528 MHz and the symbol is transmitted at a different frequency band at each block. This is why it is called multiband.

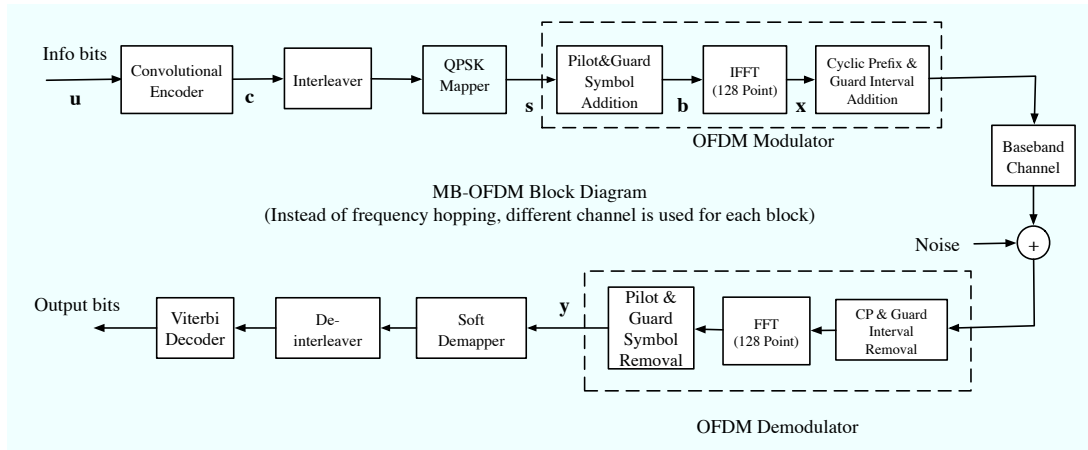


Figure 5.1. MB OFDM system model proposed in [35].

A length L_u input data stream u with elements $u_i \in \{0, 1\}$ for $i = 1, \dots, L_u$ are fed to a convolutional encoder and interleaver sequentially to create c which has 2-bit elements $c_k = [c_{k,1}c_{k,2}] \in \{-1, 1\}^2$. Then, c_k are mapped to QPSK symbol sequence $S_k \in \mathcal{S}$ for $k = 0, \dots, L_s - 1$ and $\mathcal{S} = \{e^{j\pi/4}, e^{j3\pi/4}, e^{j5\pi/4}, e^{j7\pi/4}\}$ as it is proposed in [35]. Placing pilot and guard symbols to \mathbf{S} according to [35], we obtain \mathbf{B} vector which is ready for inverse FFT.

We can obtain inverse Fourier transform of \mathbf{B} by multiplying it with inverse of Fourier transform matrix F such that $[\mathbf{F}]_{kl} = \xi^{kl}$ with $\xi = e^{-j2\pi/N}$, $j = \sqrt{-1}$ and $k, l = 0, \dots, N - 1$. N is the number of FFT points. Therefore we can obtain

$$\mathbf{x} = \mathbf{F}^{-1}\mathbf{B}. \quad (5.1)$$

Time domain discrete signal \mathbf{x} is called an OFDM block. As proposed in [35], a cyclic prefix (CP) of length L_{cp} is pre-appended and a guard interval (GI) of length- L_g is appended to the end of it as shown in Figure 5.2. By using CP, the interaction between channel and the transmitted signal becomes circular convolution. The CP is the last length- L_{cp} portion of \mathbf{x} which must be longer than the length of the channel. This fact ensures that channel's and signal's discrete Fourier transforms are multiplied. In addition, CP also removes interference from previous OFDM symbol, because it is removed at the receiver. On the other hand, the guard interval is all zeros. After adding CP and guard interval, the OFDM blocks are transmitted as modulated to appropriate frequency. For analysis purposes, we model our system at baseband. The channel model is also baseband equivalent. The transmitted signal with CP and GI added is denoted as $\tilde{\mathbf{x}}$.

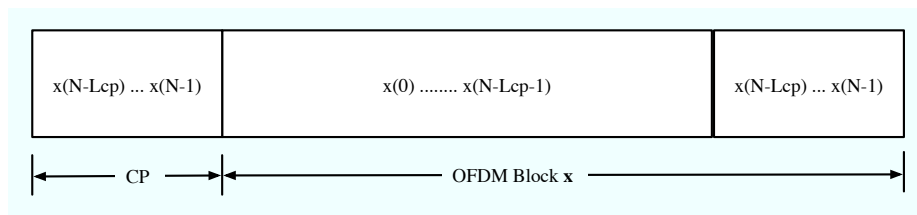


Figure 5.2. Cyclic prefix and the OFDM symbol.

The signal passes through the channel $h[n]$ which is the discrete-time baseband channel impulse response with length L and additive white Gaussian noise (AWGN) $\eta[n]$ is added. Discrete-time baseband channel impulse response is obtained from the UWB channel model used in standards by IEEE in [8] which is derived from the Saleh-Valenzuela (S-V) model [36]. The time domain impulse response of the i -th realization of the channel can be defined as

$$h_i(t) = \chi \sum_{l=0}^L \sum_{k=0}^K \alpha_{k,l}^i \delta(t - T_l^i - \tau_{k,l}^i) \quad (5.2)$$

where $\alpha_{k,l}^i$ is the multipath gain coefficients, T_l^i is the delay of the l -th cluster, and $\tau_{k,l}^i$ is the delay of the k -th multipath component within the l -th cluster relative to T_l^i . χ is the log-normal shadowing coefficient. χ is ignored because we compare the cooperation scenarios under same conditions. It only introduces a scaling of SNR. The channel characteristics and the distributions of parameters can be found in [8]. It also

includes discrete time implementation issues.

MB-OFDM uses 528 MHz wide sub-bands of UWB spectrum, so we can filter and convert those sub-bands to baseband [37]. Then we can down-sample them since the new bandwidth is not the all UWB spectrum but a 528 MHz band. The resulting baseband equivalent channel is denoted by $h[n]$.

The received signal in baseband can be written as

$$\tilde{y}[n] = \sum_{l=0}^L h[l]\tilde{x}[n-l] + \tilde{\eta}[n] \quad (5.3)$$

where $\tilde{\eta}[n]$ is complex additive white Gaussian noise with two-sided power spectral density $N_0/2$. Note that the variance of complex noise at subcarriers is still $N_0/2$. If we write them as vectors after removing the CP and GI and assuming $L_{cp} \geq L$, we get

$$\bar{y} = Hx + \eta \quad (5.4)$$

where $\bar{y} = [\tilde{y}(L_{cp}) \cdots \tilde{y}(N + L_{cp} - 1)]^T$, $x = [x(0) \cdots x(N - 1)]^T$ and

$$H = \begin{bmatrix} h(0) & 0 & \cdots & h(L-1) & \cdots & h(1) \\ h(1) & h(0) & \cdots & \cdots & \ddots & \vdots \\ \vdots & \cdots & \ddots & \cdots & \cdots & h(L-1) \\ h(L-1) & \cdots & \cdots & \ddots & \cdots & 0 \\ \vdots & \ddots & \cdots & \cdots & \ddots & \vdots \\ 0 & \cdots & h(L-1) & \cdots & \cdots & h(0) \end{bmatrix}. \quad (5.5)$$

Since $N \times N$ H is a circulant matrix, we can decompose it as $H = F^H \bar{\Lambda} F$ where F is the Fourier transform matrix. $\bar{\Lambda}$ is the diagonal matrix with Fourier transform

coefficients of h at the diagonal elements such that

$$\bar{\Lambda}[n] = \sum_{k=0}^{L-1} h[k] e^{-j \frac{2\pi kn}{N}}.$$

Multiplying the received symbol sequence \bar{y} with F , following result is obtained

$$\begin{aligned} \bar{Y} = F\bar{y} &= FHx + F\eta \\ &= FF^H \bar{\Lambda} Fx + F\eta \\ &= \bar{\Lambda} Fx + F\eta \\ &= \bar{\Lambda} B + F\eta \end{aligned} \tag{5.6}$$

which is same as multiplying the transmitted signal's Fourier transform Fx with channel's Fourier transform coefficients. Finally, we remove the symbols which belongs to pilot and guard symbols and get

$$Y = \Lambda S + N \tag{5.7}$$

where Λ is the diagonal channel coefficient matrix for carrier frequencies of data symbols and N is the complex noise vector at corresponding subcarriers. 1-tap equalizer Λ^{-1} is applied to the received sequence Y and estimates of S are calculated as

$$\hat{S} = \Lambda^{-1} Y = S + \Lambda^{-1} N. \tag{5.8}$$

After calculating the log-probabilities of S estimates, log-probabilities are fed to Viterbi decoder.

6. SPACE TIME CODED UWB COOPERATION

Cooperation using MB-OFDM is performed as cooperative data transmission of two users as shown in Figure 6.1. First, the users share their data and decode their partners' signal. Then, they transmit the signals in a distributed ST coded scheme. Since the partners can decode erroneously, the cooperation performance becomes limited proportionally to the inter-user channel performance.

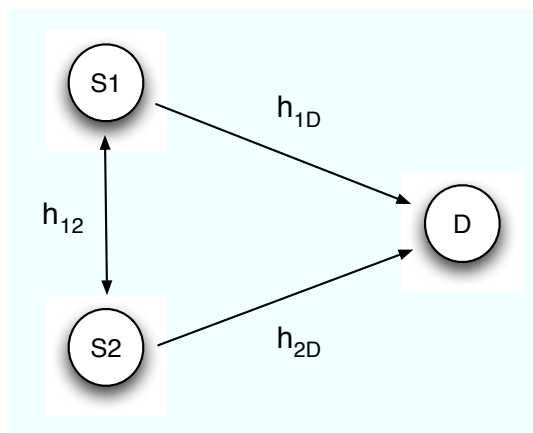


Figure 6.1. Two user cooperation model.

Assume two users want to transmit QPSK symbols $S_1(i)$ and $S_2(i)$. Those symbols are mapped from the output of convolutional encoder. For cooperation, they first transmit symbols to their partners in first time slot. Each user decodes the partner's data correctly or with some errors. Since they use hard decisions, the system is called STCC with hard decoding (STCC-hard). Then, they use the data they decoded to transmit the symbols $-\tilde{S}_2^*(i)$ and $-\tilde{S}_1^*(i)$ in second time slot, where * means complex conjugate and \tilde{S}_i is symbol mapped from the decisions on c_j at partner. This scheme is the well known Alamouti ST code [1]. The symbols transmitted in second time slot are the decoded versions of original symbols and they can be erroneous. The symbols are transmitted using MB-OFDM system. At the receiver, the received signals at two

time slots after OFDM demodulation are

$$\begin{aligned} Y_1 &= \Lambda_{11}S_1 + \Lambda_{12}S_2 + N_1, \\ Y_2 &= -\Lambda_{21}\tilde{S}_2^* + \Lambda_{22}\tilde{S}_1^* + N_2, \end{aligned} \quad (6.1)$$

where Λ_{ij} are the FFT coefficients of channels from user j to destination and N_i are the FFT coefficients of noise at time slot i . We can model \tilde{S}_i 's as a noisy symbol with noise e such that

$$\tilde{S}_i = S_i + e_i, \quad i = 1, 2. \quad (6.2)$$

Assuming quasi-static channels, such that $\Lambda_{21} = \Lambda_{11}$ and $\Lambda_{12} = \Lambda_{22}$, and applying ST decoding, the symbol estimates at the destination become

$$\hat{S}_1 = (|\Lambda_{11}|^2 + |\Lambda_{22}|^2)S_1 + |\Lambda_{22}|^2e_1 - \Lambda_{11}^*\Lambda_{22}e_2 + \Lambda_{11}^*N_1 + \Lambda_{22}N_2^*, \quad (6.3)$$

$$\hat{S}_2 = (|\Lambda_{11}|^2 + |\Lambda_{22}|^2)S_2 + |\Lambda_{11}|^2e_2 - \Lambda_{11}\Lambda_{22}^*e_1 + \Lambda_{22}^*N_1 - \Lambda_{11}N_2^*. \quad (6.4)$$

As we can see, we have an additional distortion of e_i which is a result of interuser communication. The received SNR of the system for user 1's data can be calculated as

$$\gamma_{d1} = \frac{(|\Lambda_{11}|^2 + |\Lambda_{22}|^2)^2 E_b / 2}{|\Lambda_{22}|^4 \sigma_{e_1}^2 + |\Lambda_{11}|^2 |\Lambda_{22}|^2 \sigma_{e_2}^2 + |\Lambda_{11}|^2 \sigma_{N_1}^2 + |\Lambda_{22}|^2 \sigma_{N_2}^2} \quad (6.5)$$

where γ represents SNR. While our symbols are QPSK, $e \in \{0, \pm\sqrt{2}, \pm\sqrt{2}j, \pm\sqrt{2} \pm \sqrt{2}j, \mp\sqrt{2} \pm \sqrt{2}j\}$. Using interleaver helps us to take bit errors equiprobable and thus we can generate the probability distribution of e_i . We can also assume that e_1 and e_2 have the same statistical properties such as mean and variance so we can drop the index. The noise samples n_i are also have same statistical properties where $N_i = F\eta_i$. All e_i and N_i are assumed to be independent. With the assumptions above, the Equation 6.5

becomes

$$\gamma_{d1} = \frac{(|\lambda_{11}|^2 + |\lambda_{22}|^2)E_b/2}{|\lambda_{22}|^2\sigma_e^2 + \sigma_N^2}. \quad (6.6)$$

We can see that the error is transferred to destination through the channel between user 2 and the destination. This is intuitively correct that e is the decoding error of user 1's data at user 2. A similar equation can be written for user 2 such that

$$\gamma_{d2} = \frac{(|\Lambda_{11}|^2 + |\Lambda_{22}|^2)E_b/2}{|\Lambda_{11}|^2\sigma_e^2 + \sigma_N^2}. \quad (6.7)$$

The probabilities for e are presented in Table 6.1 where P_b is the bit error probabilities of the bits which select the QPSK symbol. The mean and variance of e can be calculated as 0 and $4P_b$ respectively.

Table 6.1. Probability distribution of inter-user symbol error e

e	$P(e)$
0	$(1 - P_b)^2$
$\sqrt{2}$	$(1 - P_b)P_b/2$
$-\sqrt{2}$	$(1 - P_b)P_b/2$
$j\sqrt{2}$	$(1 - P_b)P_b/2$
$-j\sqrt{2}$	$(1 - P_b)P_b/2$
$\sqrt{2} + j\sqrt{2}$	$P_b^2/4$
$\sqrt{2} - j\sqrt{2}$	$P_b^2/4$
$-\sqrt{2} + j\sqrt{2}$	$P_b^2/4$
$-\sqrt{2} - j\sqrt{2}$	$P_b^2/4$

We introduce three solutions to improve the performance and lower the error floor. First step is using soft symbols instead of QPSK symbols in cooperation period. The second alternative is employing iterative turbo decoding at partners. The last one is using CRC code to decide on cooperation.

6.1. Cooperation with Soft Decoding

To decrease the effect of hard decision errors on cooperation, we introduce STCC with soft decoding (STCC-soft). The users calculate soft information of their partners' data and generates a soft symbol from it. Introducing iteration to this system, i.e. performing more than one transmission during share of data between users, we obtain performance gains. In [10], a similar system with amplify-and-forward (AF) cooperation is introduced with BPSK modulation and Rayleigh block fading channels.

In that soft decision scheme, users transmit their information to their partners before cooperation. At the partners, the LLRs are not converted to hard decisions but they are used to transmit soft symbols created by soft bits. The soft bit corresponding to $c_{k,l}$ can be created from the output LLRs in Equation 4.20 such that

$$\bar{c}_{k,l} = \frac{e^{L(c_{k,l})} - 1}{e^{L(c_{k,l})} + 1} = \tanh \frac{L(c_{k,l})}{2} \quad (6.8)$$

and the soft symbols are generated from soft bits by

$$\bar{S}_k = \frac{1}{\sqrt{2}}(\bar{c}_{k,1} + j\bar{c}_{k,2}). \quad (6.9)$$

Finally, the soft symbols are fed to output of QPSK Mapper and partners transmit \bar{S} instead of \tilde{S} in Equation 6.2.

The performance of soft cooperation shows a trend similar to hard decision cooperation. But the error floor is lower than the hard decision. If we denote the error of the symbol transmitted by e' , we obtain a similar expression with Equation 7.4. Since e' is the difference between the actual symbol and the soft symbol, it can be written as

$$\begin{aligned} e' &= \frac{1}{\sqrt{2}}(c_{k,1} + jc_{k,2}) - \frac{1}{\sqrt{2}}(\bar{c}_{k,1} + j\bar{c}_{k,2}) \\ &= \frac{1}{\sqrt{2}} \left(\left[c_{k,1} - \tanh \left(\frac{L(c_{k,1})}{2} \right) \right] + j \left[c_{k,2} - \tanh \left(\frac{L(c_{k,2})}{2} \right) \right] \right) \quad (6.10) \end{aligned}$$

The variance of e' becomes

$$\begin{aligned}
\sigma_{e'}^2 &= \frac{1}{2}E \left[\left(c_{k,1} - \tanh \left[\frac{L(c_{k,1})}{2} \right] \right)^2 + \left(c_{k,2} - \tanh \left[\frac{L(c_{k,2})}{2} \right] \right)^2 \right] \\
&\leq \frac{1}{2}E \left[\left(c_{k,1} - \text{sign} \left[\frac{L(c_{k,1})}{2} \right] \right)^2 \right] + \frac{1}{2}E \left[\left(c_{k,2} - \text{sign} \left[\frac{L(c_{k,2})}{2} \right] \right)^2 \right] \\
&= \sigma_e^2
\end{aligned} \tag{6.11}$$

The tanh is bounded between 1 and -1 at extremes. For weak values of $L(c_{k,1})$ and $L(c_{k,2})$, the soft symbol is closer to 0, resulting in a smaller error. On the other hand, hard decision maps the wrong bits to a QPSK symbol which is far away from the actual symbol.

6.2. Cooperation with Iterative Decoding

STCC with iterative decoding (STCC-ID) uses iterative decoding at the cooperating users. The information bits of each user are first convolutionally encoded and an iterative demapper-decoder which is explained in Section 4.2 is employed instead of Viterbi decoder at partners as shown in Figure 6.2. It is shown in [34] that we can obtain substantial gains by employing iterative decoding. This system can be implemented with both STCC-hard and STCC-soft. The result is a better inter-user channel performance and a better cooperation error rate since σ_e becomes lower. This can be seen from Extrinsic Information Transfer (EXIT) chart in Figure 4.4 as the increase of mutual information.

6.3. Cooperation with CRC

We can introduce CRC control to each of the above schemes. After information sharing, the users control the CRC of their partners bits and decide if they can cooperate. If the CRC check fails, they do not cooperate and transmit their signals separately. This is important at the point where the error floor stays above single user performance. That scheme can prevent limiting factor of inter-user channel and we

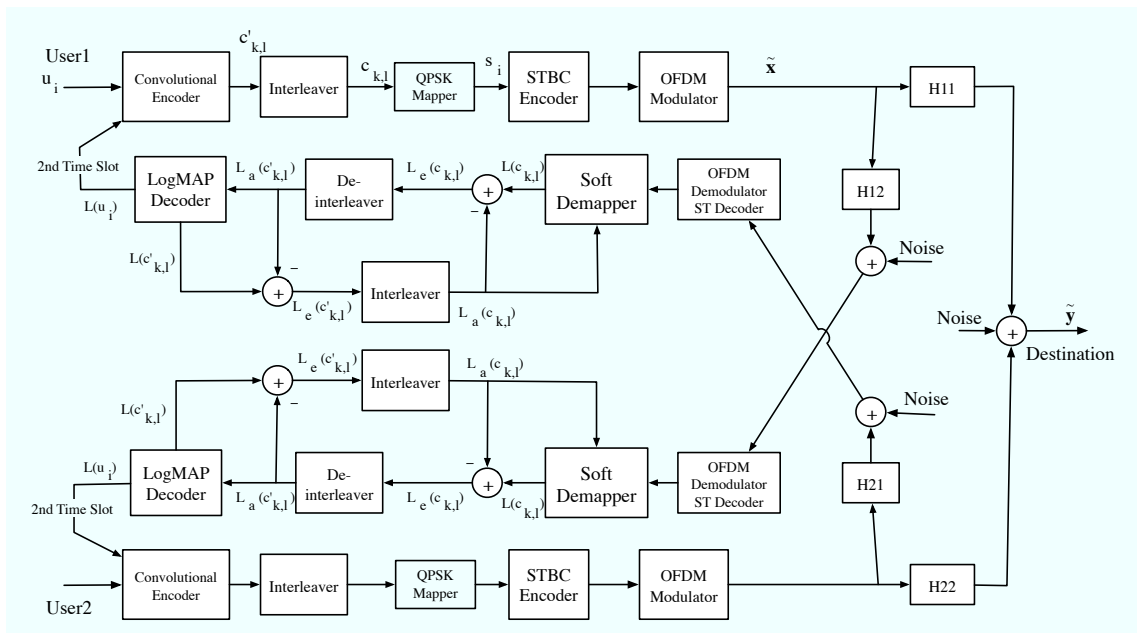


Figure 6.2. STCC with iterative decoding system model.

obtain a performance between single user (SU) transmission and full ST cooperation with perfect inter-user channel.

7. ERROR PERFORMANCE ANALYSIS

7.1. Performance of User Cooperative MB-OFDM without CRC

The performance analysis of hard and soft decision cooperation are same except the variance of e . For the appropriate result, we can replace σ_e with $\sigma_{e'}$.

In [38], the bit error rate of an uncoded 2x1 system is derived as

$$P_e^{2x1} = E \left\{ Q \left(\sqrt{\frac{2(|\Lambda_{11}|^2 + |\Lambda_{22}|^2) E_b}{N_0}} \right) \right\} \quad (7.1)$$

where Λ_{ii} are statistically independent and circularly Gaussian distributed with $E\{|\Lambda_{11}|^2\} = E\{|\Lambda_{22}|^2\} = 1$ and E_b is the energy per bit. The expectation [38] results in

$$P_e^{2x1} = \frac{1}{2} - \frac{3}{4}\mu + \frac{1}{4}\mu^3 \quad (7.2)$$

with

$$\mu = \sqrt{\frac{0.5\gamma_r}{1 + 0.5\gamma_r}}. \quad (7.3)$$

It is easy to integrate the above expectation via using the method in [39]. But we have Equation 6.6 inside the Q -function. The BER for STCC with hard decoding is

$$P_e^{STCC} = E \left\{ Q \left(\sqrt{\frac{2(|\Lambda_{11}|^2 + |\Lambda_{22}|^2) E_b}{|\Lambda_{22}|^2 \sigma_e^2 + N_0}} \right) \right\} \quad (7.4)$$

Since $|\Lambda_{11}|^2$ and $|\Lambda_{22}|^2$ are statistically independent and we also have a $|\Lambda_{22}|^2$ term in the denominator, we have to calculate expectation via computing the integrals. The

result is (see Appendix B for derivation)

$$P_e^{STCC}(\gamma) = \frac{1}{\pi} \int_0^{\pi/2} \left[\int_0^\infty \exp\left(-\frac{\alpha E_b}{(\alpha\sigma_e^2 + N_0) \sin^2 \theta}\right) \frac{(\alpha\sigma_e^2 + N_0) \sin^2 \theta}{(\alpha\sigma_e^2 + N_0) \sin^2 \theta + E_b \bar{\gamma}} \frac{e^{-\alpha/\bar{\gamma}}}{\bar{\gamma}} d\alpha \right] d\theta \quad (7.5)$$

which can be evaluated numerically. In Equation 7.5, $\alpha = |\Lambda_{11}|^2$ and $\beta = |\Lambda_{22}|^2$. The results in Figure 7.1 show that the performance has the error floor we mentioned. In Figure 7.2, the theoretical results are calculated for symmetrical channel conditions such that distances between users and destination are similar and the channel is CM1. There is not an error floor in that situation because the error between users changes with changing SNR.

7.2. Performance of User Cooperative MB-OFDM with CRC

The bit error rate of the user cooperation system with CRC can be calculated as

$$P_e^{CRC} = (1 - P_f)P_e^{2x1} + P_f P_e^{SU} \quad (7.6)$$

where P_e^{SU} is the bit error rate for single antenna communication. P_f denotes the probability that the frame is decoded erroneously. The users cooperate when they correctly decode each others data.

The single antenna bit error rate (BER) for MB OFDM system without coding is given in [38] as

$$P_e^{SU}(\gamma_r) = \frac{1}{2} \left(1 - \sqrt{\frac{\gamma_r}{1 + \gamma_r}} \right) \quad (7.7)$$

where $\gamma_r = E_b/N_0$ is the received signal-to-noise ratio at the receiver. The probability that a frame with length N_b is decoded erroneously is

$$P_f = 1 - (1 - P_e^{SU}(\gamma_r))^{N_b}. \quad (7.8)$$

The final result is

$$\begin{aligned}
 P_e^{CRC}(\gamma_{sr}, \gamma_d) &= P_f P_e^{SU} + (1 - P_f) P_e^{ST} \\
 &= (1 - (1 - P_e^{SU}(\gamma_{sr}))^{N_b}) \frac{1}{2} \left(1 - \sqrt{\frac{\gamma_d}{1 + \gamma_d}} \right) \\
 &\quad + (1 - P_e^{SU}(\gamma_{sr}))^{N_b} \left(\frac{1}{2} - \frac{3}{4} \mu + \frac{1}{4} \mu^3 \right). \tag{7.9}
 \end{aligned}$$

We can see the results for system employing CRC in Figure 7.1 and Figure 7.2. CRC prevents error floor when inter-user channel SNR is assumed fixed.

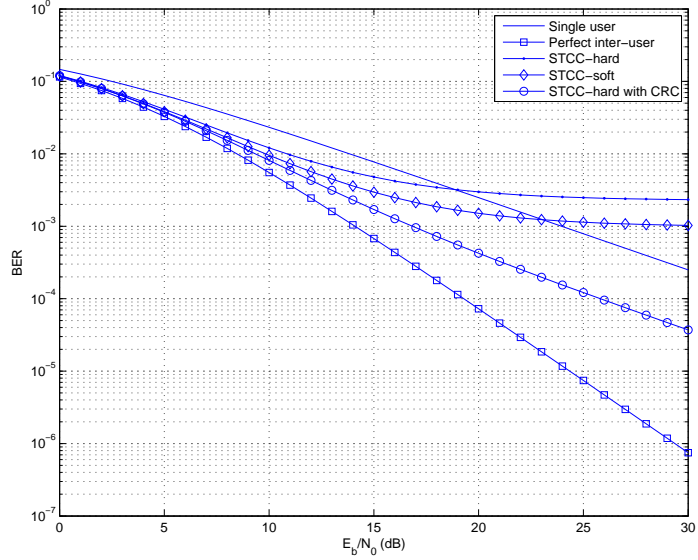


Figure 7.1. Theoretical BER for uncoded STCC schemes at 20dB CM1 inter-user channel.

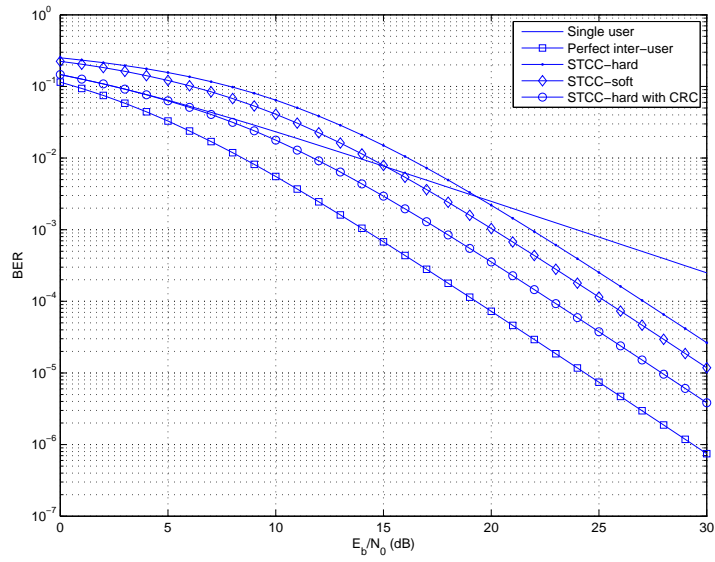


Figure 7.2. Theoretical BER for uncoded STCC schemes symmetrical channel conditions in between users and destination.

8. SIMULATIONS AND RESULTS

In this section, the proposed UWB cooperative systems are simulated under IEEE UWB channels [8]. We employed rate-1/2 punctured convolutional code for iterative STCC, the output of which is interleaved and mapped to QPSK symbols. The generator polynomials for encoder are (133, 145, 175) in octal representation. Then the complex symbols are passed through 128-point IFFT. Baseband signal model is used and the channel is changed for time slots to obtain multi-band effect. For the simulations, a symmetrical positioning is used such that the channels between partners and from partners to destination have similar channel characteristics and SNR. We assume that both the users and the destination have perfect channel state information (CSI). The channels are generated and converted to their baseband equivalents according to [8]. For the systems using CRC, we used a length-12 CRC code with generator polynomial $x^{12} + x^{11} + x^3 + x^2 + x + 1$ [40].

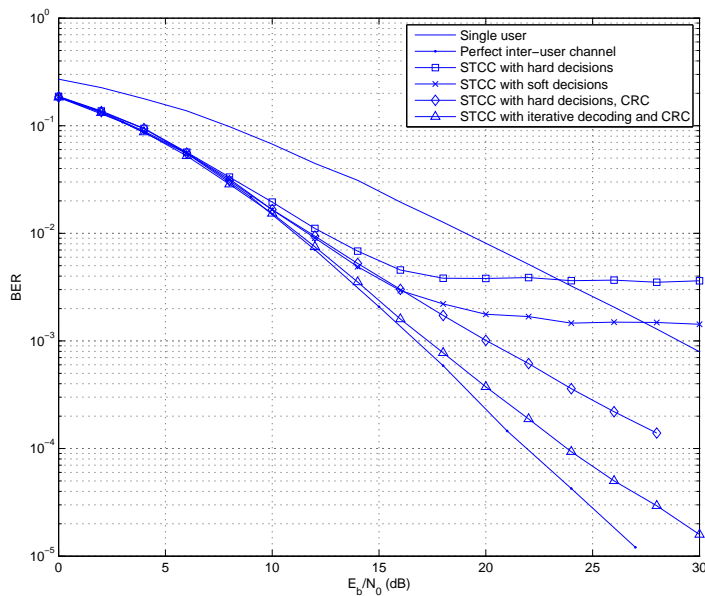


Figure 8.1. Simulation results for proposed ST coded MB OFDM cooperation scenarios with 20dB inter-user SNR.

The curves in Figure 7.1 shows the theoretical performance of STCC with hard decision, soft decision and hard decision employing CRC. Since the interuser channel

is bad, the erroneous decoding increases the error rate of the system. Although we cannot reach to ST coded MB-OFDM performance, we obtain better error rates than single user transmission by employing CRC. Soft symbol cooperation with CRC is not included because the system with CRC uses the hard decisions for CRC control. We see that cooperation is helpful to improve performance when inter-user channel performance in the system is better than user-to-destination channel. In Figure 8.1 and Figure 8.2, we compare the simulation results of the scenarios for fixed inter-user channel SNR. The results are compatible with theoretical analysis and proves that BER becomes lower than single user case when inter-user channel is in good condition according to user-to-destination channel. CRC helps us to have a parallel but lower BER curve than single user because when there is error in inter-user channel communication, the users do not cooperate. If decoding at partners is correct, they get a ST code performance. On the average, we obtain a performance between single user and ST coding BERs.

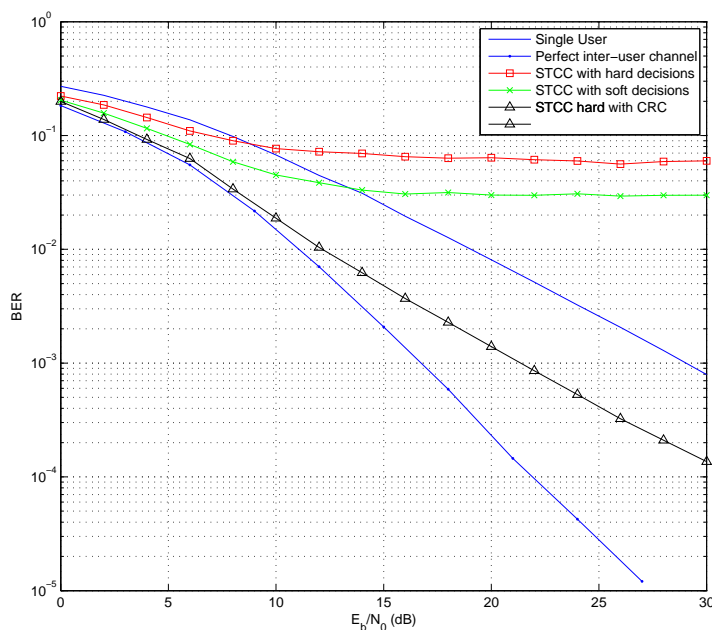


Figure 8.2. Simulation results for proposed ST coded MB OFDM cooperation scenarios with 10dB inter-user SNR.

Figure 8.3 represents the simulation performance when there is a symmetrical positioning of users and the destination. The inter-user SNR is kept same as the user-destination channel SNR and performance is calculated with respect to user-destination

SNR. We get a better performance by employing soft decision and CRC codes. STCC with CRC is parallel to STCC with perfect inter-user channel in this case because SNR for inter-user channel also increases in addition to user-to-destination channel with respect to fixed SNR situation presented above.

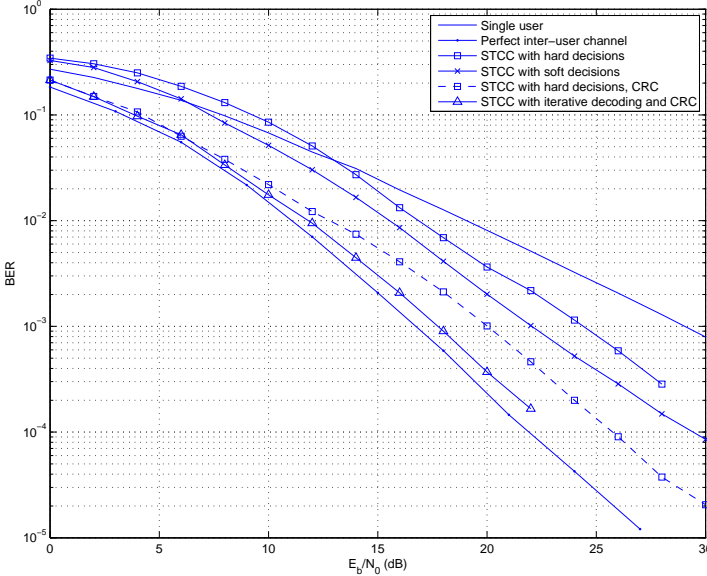


Figure 8.3. Simulation results of proposed ST coded MB-OFDM cooperation systems in symmetrical channel conditions.

In Figure 8.4, we compared two iterative detection schemes, one without CRC and one with CRC. Partners perform two iterations to decode the signal they received from their collaborator. We compared the performance against coded single user case and coded ST coded case with perfect inter-user channel. While STCC with iterative decoding results in error floor, introducing CRC, we perform as well as STCC with perfect inter-user channel especially in mid-SNR values.

Finally, the Figure 8.5 shows the performance of STCC with iterative decoding across CM3 channels. The inter-user channel is still fixed at CM1 20dB but the channel between users and destination is CM3. The result is very close to that of CM1 user-destination channel because we ignored the log-normal fading coefficient and normalized the channel coefficients.

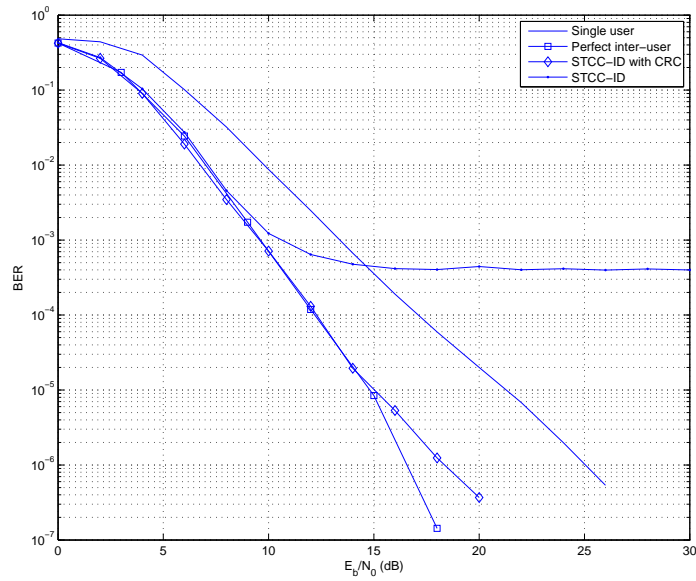


Figure 8.4. Simulation results for STCC-ID with and without CRC at 20dB inter-user SNR.

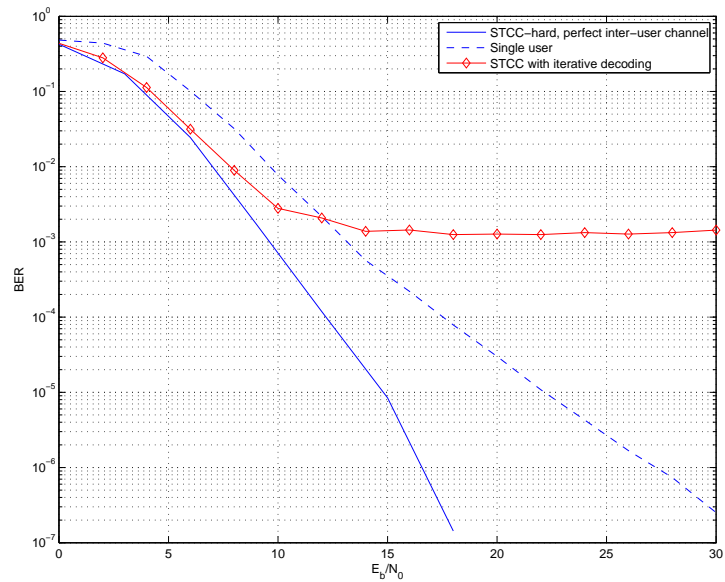


Figure 8.5. Simulation results for STCC-ID at 20dB CM1 inter-user SNR. The user-destination channel is CM3.

9. CONCLUSIONS

In this study, we proposed ST coded cooperation techniques to use with UWB MB-OFDM systems. ST cooperation is a simple but powerful method to obtain higher performance when users-to-destination channel is severe. Theoretical analysis and the simulation results show that the inter-user channel condition is highly effective on cooperation performance. We obtain error floors due to that errors. However, it is shown that performance can be boosted by usage of ST cooperation with iterative decoding at partners. Also, CRC code is an effective tool to prevent error floors due to inter-user channel performance, if we use it to decide on cooperation. When the need for simplicity of partners increases, soft information aided scheme can also be used.

Our study shows that the users can improve their communication performance using ST cooperation techniques when their inter-user channel performance, i.e. BER, is better than the performance of the channel between them and destination. The decision on which channel is better can be made by some feedback mechanism between users and destination which is not implemented in our work.

**APPENDIX A: DERIVATION OF EXTRINSIC LLR IN
EQUATION 4.21**

The LLR of $c_{k,l}$ is derived as

$$\begin{aligned}
L(c_{k,l}) &= \log \frac{P(c_{k,l} = 1|Y_k)}{P(c_{k,l} = -1|Y_k)} = \log \frac{\sum_{\forall S_k: c_{k,l}=1} P(Y_k|S_k)P(s)}{\sum_{\forall S_k: c_{k,l}=-1} P(Y_k|S_k)P(S_k)} \\
&= \log \frac{\sum_{\forall S_k: c_{k,l}=1} \exp(K(S_k)) \prod_{m=1}^2 P(c_{k,m})}{\sum_{\forall S_k: c_{k,l}=-1} \exp(K(S_k)) \prod_{m=1}^2 P(c_{k,m})} \\
&= \log \frac{\sum_{\forall S_k: c_{k,l}=1} \exp(K(S_k)) P(c_{k,l} = 1) P(c_{k,m})}{\sum_{\forall S_k: c_{k,l}=-1} \exp(K(S_k)) P(c_{k,l} = -1) P(c_{k,m})} \\
&= \log \frac{P(c_{k,l} = 1)}{P(c_{k,l} = -1)} + \log \frac{\sum_{\forall S_k: c_{k,l}=1, l \neq m} \exp(K(S_k) + \log P(c_{k,m}))}{\sum_{\forall S_k: c_{k,l}=-1, l \neq m} \exp(K(S_k) + \log P(c_{k,m}))} \\
&= L_a(c_{k,l}) + \log \frac{\sum_{\forall S_k: c_{k,l}=1, l \neq m} \exp(K(S_k) + \frac{1}{2} c_{k,m} L_a(c_{k,m}))}{\sum_{\forall S_k: c_{k,l}=-1, l \neq m} \exp(K(S_k) + \frac{1}{2} c_{k,m} L_a(c_{k,m}))} \\
&= L_a(c_{k,l}) + L_e(c_{k,l}) \tag{A.1}
\end{aligned}$$

where $K(s_k)$ is defined in Equation 4.22.

APPENDIX B: DERIVATION OF EQUATION 7.5

In Equation 7.1, the sum $x = \sum_l |\Lambda_{ll}|^2$ is chi-square distributed, with the probability density function (pdf)

$$f(x) = \frac{1}{(K-1)!} x^{K-1} e^{-x} \quad (\text{B.1})$$

where K is the number of $|\Lambda_{ll}|^2$ terms in the sum. Taking the expectation of Equation 7.1 with respect to Equation B.1 gives the result in Equation 7.2. It is easy to integrate Equation 7.1 via using the method in [39]. But we have Equation 6.6 inside the Q -function. The probability density distribution of $x_i = |\Lambda_{ii}|^2$ can be written as

$$f(x_i) = \frac{1}{2\sigma_{x_i}^2} e^{-x_i/\sigma_{x_i}^2}. \quad (\text{B.2})$$

Averaging Gaussian Q-function

The BER for a communication system is generally calculated as a Q -function given the channel coefficients. We need to average the BER over all possible channels. An alternative form of Q -function which is defined in [39] is used in averaging such that

$$Q(x) = \frac{1}{\pi} \int_0^{\pi/2} \exp\left(-\frac{x^2}{2\sin^2\theta}\right) d\theta. \quad (\text{B.3})$$

The expectation of Q -function over channel coefficient distributions is derived as follows:

$$\begin{aligned}
P_e = E_\gamma[Q(a\sqrt{\gamma})] &= \int_0^\infty Q(a\sqrt{\gamma})p_\gamma(\gamma)d\gamma \\
&= \int_0^\infty \frac{1}{\pi} \int_0^{\pi/2} \exp\left(-\frac{a^2\gamma}{2\sin^2(\theta)}\right)d\theta p_\gamma(\gamma)d\gamma \\
&= \frac{1}{\pi} \int_0^{\pi/2} \left[\int_0^\infty \exp\left(-\frac{a^2\gamma}{2\sin^2(\theta)}\right)p_\gamma(\gamma)d\gamma \right] d\theta. \quad (\text{B.4})
\end{aligned}$$

Since the moment generating function (MGF) of a pdf is defined as $M_\gamma(s) = \int_0^\infty e^{s\gamma}p_\gamma(\gamma)d\gamma$, the integral in Equation B.4 results in

$$P_e = \frac{1}{\pi} \int_0^{\pi/2} M_\gamma\left(-\frac{a^2}{2\sin^2(\theta)}\right) d\theta. \quad (\text{B.5})$$

But we have Equation 7.4 as the probability of error. We cannot evaluate Equation 7.4 directly with Equation B.5 because we also have a $|\Lambda_{11}|^2$ term in the denominator. To calculate the above expectation, we use the alternative form of Q-function and integrate over two pdfs which results in Equation 7.5 as follows:

$$\begin{aligned}
P_e(\gamma) &= \int_0^\infty \int_0^\infty \frac{1}{\pi} \int_0^{\pi/2} \exp\left(-\frac{\frac{2(\alpha+\beta)E_b}{\alpha\sigma_e^2+N_0}}{2\sin^2\theta}\right)d\theta \frac{e^{-\alpha/\bar{\gamma}}}{2\bar{\gamma}}d\alpha \frac{e^{-\beta/\bar{\gamma}}}{2\bar{\gamma}}d\beta \\
&= \frac{1}{4\pi} \int_0^{\pi/2} \left[\int_0^\infty \int_0^\infty \exp\left(-\frac{(\alpha+\beta)E_b}{(\alpha\sigma_e^2+N_0)\sin^2\theta}\right) \frac{e^{-\alpha/\bar{\gamma}}e^{-\beta/\bar{\gamma}}}{\bar{\gamma}^2}d\alpha d\beta \right] d\theta \\
&= \frac{1}{4\pi} \int_0^{\pi/2} \left[\int_0^\infty \exp\left(-\frac{\alpha E_b}{(\alpha\sigma_e^2+N_0)\sin^2\theta}\right) \frac{e^{-\alpha/\bar{\gamma}}}{\bar{\gamma}} \left\{ M_\beta\left(\frac{E_b}{(\alpha\sigma_e^2+N_0)\sin^2\theta}\right) \right\} d\alpha \right] d\theta \\
&= \frac{1}{4\pi} \int_0^{\pi/2} \left[\int_0^\infty \exp\left(-\frac{\alpha E_b}{(\alpha\sigma_e^2+N_0)\sin^2\theta}\right) \frac{e^{-\alpha/\bar{\gamma}}}{\bar{\gamma}} \left\{ \frac{1}{1 + \frac{E_b\bar{\gamma}}{(\alpha\sigma_e^2+N_0)\sin^2\theta}} \right\} d\alpha \right] d\theta \quad (\text{B.6})
\end{aligned}$$

$$= \frac{1}{4\pi} \int_0^{\pi/2} \int_0^\infty \exp\left(-\frac{\alpha E_b}{(\alpha\sigma_e^2+N_0)\sin^2\theta}\right) \frac{(\alpha\sigma_e^2+N_0)\sin^2\theta}{(\alpha\sigma_e^2+N_0)\sin^2\theta + E_b\bar{\gamma}} \frac{e^{-\alpha/\bar{\gamma}}}{\bar{\gamma}} d\alpha d\theta \quad (\text{B.7})$$

where

$$M_\beta\left(\frac{E_b}{(\alpha\sigma_e^2+N_0)\sin^2\theta}\right) = \int_0^\infty \exp\left(-\frac{E_b}{(\alpha\sigma_e^2+N_0)\sin^2\theta}\beta\right) \frac{e^{-\beta/\bar{\gamma}}}{\bar{\gamma}} d\beta. \quad (\text{B.8})$$

Equation B.8 is the MGF of β which is Rayleigh-distributed.

REFERENCES

1. S. M. Alamouti, "A Simple Transmit Diversity Technique for Wireless Communications", *IEEE Journal on Selected Areas in Communications*, Vol.16, pp. 1451-1458, October 1998.
2. J. N. Laneman, G. W. Wornell, "Distributed Space-Time Coded Protocols for Exploiting Cooperative Diversity in Wireless Networks", *IEEE Transactions on Information Theory*, Vol. 49, pp. 2415-2425, October 2003.
3. X. Li, M. Chen, W. Liu, "Application of STBC-Encoded Cooperative Transmission in Wireless Sensor Networks", *IEEE Signal Processing Letters*, Vol. 12, No. 2, pp. 134-137, February 2005.
4. A. Sendonaris, E. Erkip, B. Aazhang, "User Cooperation Diversity - Part 1: System Description", *IEEE Transactions on Communications*, Vol. 51, No. 11, pp. 1927-1938, November 2003.
5. A. Sendonaris, E. Erkip, B. Aazhang, "User Cooperation Diversity - Part 2: Implementation Aspects and Performance Analysis", *IEEE Transactions on Communications*, Vol. 51, No. 11, pp. 1939-1948, November 2003.
6. J. Niu, I-T. Lu, "Coded Cooperation in OFDMA Systems", in *Proceedings of 40th Annual Conference on Information Sciences and Systems*, 22 - 24 March 2006, pp. 300-305, 2006.
7. S. Barbarossa, G. Scutari, "Distributed Space-Time Coding Strategies for Wideband Multihop Networks: Regenerative vs. Non-regenerative Relays", in *Proceedings of IEEE International Conference on Acoustics, Speech, and Signal Processing*, 17-21 May 2004, Vol. 4, pp. iv-501-504, 2004.
8. "Channel Modeling Sub-committee Report Final", IEEE 802.15-02/490r1-SG3a,

February 2003.

9. S. Dehnie, H. T. Sencar, N. Memon, "Cooperative Diversity in the Presence of A Misbehaving Relay: Performance Analysis", in *Proceedings of IEEE Sarnoff Symposium*, 30 April - 2 May, 2007.
10. H. H. Sneessens, L. Vandendorpe, "Soft Decode and Forward Improves Cooperative Communications", in *Proceedings of Computational Advances In Multi-Sensor Adaptive Processing*, 13-15 December 2005, pp. 157-160, 2005.
11. B. Vucetic, J. Yuan, *Space-Time Coding*, John Wiley & Sons Ltd, West Sussex, 2003.
12. J. N. Laneman, G. W. Wornell, D. N. C. Tse, "An Efficient Protocol for Realizing Cooperative Diversity in Wireless Networks", in *Proceedings of IEEE International Symposium On Information Theory*, 24 - 29 June 2001, pp. 294, 2001.
13. J. N. Laneman, D. N. C. Tse, G. W. Wornell, "Cooperative Diversity in Wireless Networks: Efficient Protocols and Outage Behavior", *IEEE Transactions On Information Theory*, Vol. 50, No. 12, pp. 3062-3080, December 2004.
14. J. Luo, R. S. Blum, L. J. Cimini, L. J. Greenstein, A. M. Haimovich, "Link-Failure Probabilities for Practical Cooperative Relay Networks," in *Proceedings of IEEE 61st Vehicular Technology Conference*, 30 May - 1 June 2005, Vol. 3, pp. 1489-1493, 2005.
15. E. Zimmerman, P. Herhold, G. Fettweis, "On the Performance of Cooperative Diversity Protocols in Practical Wireless Systems", in *Proceedings of IEEE 58th Vehicular Technology Conference*, 6 - 9 October 2003, Vol. 4, pp. 2212-2216, 2003.
16. J. Adeane, M. R. D. Rodrigues, I. J. Wassell, "Characterisation of the Performance of Cooperative Networks in Ricean Fading Channels", in *Proceedings of 12th International Conference On Telecommunications*, Cape Town, South Africa, May

- 2005.
17. N. Shastry, J. Bhatia, R. S. Adve, "Theoretical Analysis of Cooperative Diversity in Wireless Sensor Networks", in *Proceedings of IEEE Global Telecommunications Conference*, 28 November - 2 December 2005, Vol. 6, pp. 3269-3273, 2005.
 18. O. Shalvi, "Multiple Source Cooperation Diversity", *IEEE Communication Letters*, Vol. 8, No. 12, pp. 712-714, December 2004.
 19. X. Li, M. Chen, W. Liu, "Cooperative Transmission in Wireless Sensor Networks with Imperfect Synchronization", *Conference Record of the 38th Asilomar Conference On Signals, Systems And Computers*, 7-10 November 2004, Vol. 1, pp. 1281-1285, 2004.
 20. D. Gesbert, M. Shafi, D. Shan Shiu, P. J. Smith, A. Naguib, "From Theory to Practice: An Overview of MIMO Space-Time Coded Wireless Systems", *IEEE Journal On Selected Areas In Communications*, Vol. 21, No. 3, pp. 281-302, April 2003.
 21. V. Tarokh, H. Jafarkhani, A. R. Calderbank, "Space-Time Block Codes from Orthogonal Designs", *IEEE Transactions on Information Theory*, Vol. 45, No. 5, pp. 1456-1467, July 1999.
 22. H. Mheidat, M. Uysal, N. Al-Dhahir, "Time- and Frequency-Domain Equalization for Quasi-Orthogonal STBC Over Frequency-Selective Channels", in *Proceedings of IEEE International Conference On Communications*, 20-24 June 2004, Vol. 2, pp. 697-701, 2004.
 23. H. Mheidat, M. Uysal, "Equalization Techniques for Space-Time Coded Cooperative Systems", in *Proceedings of IEEE 60th Vehicular Technology Conference*, 26 - 29 September 2004, Vol. 3, pp. 1708 - 1712, 2004.
 24. H. Mheidat, M. Uysal, N. Al-Dhahir, "Distributed Space-Time Block Coded

- OFDM for Relay-Assisted Transmission”, in *Proceedings of IEEE International Conference On Communications*, June 2006, Vol. 10, pp. 4513-4519, 2006.
25. H. Mheidat, M. Uysal, N. Al-Dhahir, “Time-Reversal Space-Time Equalization for Amplify-and-Forward Relaying”, in *Proceedings of IEEE International Conference On Communications*, June 2006, Vol. 4, pp. 1705-1711, 2006.
 26. J. Niu, I-T. Lu, “Coded Cooperation in OFDMA Systems”, in *Proceedings of IEEE 40th Annual Conference On Information Sciences And Systems*, 22-24 March 2006, pp. 300-305, 2006.
 27. S. Yatawatta, A. P. Petropulu, “A Multiuser OFDM System with User Cooperation”, in *Conference Record of the 38th Asilomar Conference On Signals, Systems And Computers*, 7-10 November 2004, Vol. 1, pp. 319-323, 2004.
 28. S. Haykin, *Communication Systems*, Wiley, New Jersey, 2001.
 29. P. Elias, “Coding for Noisy Channels”, *1955 Conv. Rec.*, pt. 4, pp. 37-41, 1955.
 30. B. Reiffen, “Sequential Decoding for Discrete Input Memoryless Channels”, *IRE Transactions on Information Theory*, Vol. 8, No. 3, pp. 208-220, April 1962.
 31. J. Massey, “Coding Theory”, *IEEE Transactions on Information Theory*, Vol. 9, No. 4, pp. 223-229, October 1963.
 32. A. J. Viterbi, “Error bounds for convolutional Codes and an Asymptotically Optimal Decoding Algorithm”, *IEEE Transactions on Information Processing*, Vol. 13, pp. 260-269, 1967.
 33. L. Bahl, J. Cocke, F. Jelinek, J. Raviv, “Optimal Decoding of Linear Codes for Minimizing Symbol Error Rate”, *IEEE Transactions on Information Theory*, Vol. 20, No. 2, pp. 284-287, March 1974.
 34. S. Ten Brink, J. Speidel And R.-H. Yan, “Iterative Demapping for QPSK Modu-

- lation”, *Electronics Letters*, Vol.34, No.15, pp.1459-1460, 23 July 1998.
35. A. Batra *et al.*, “Multi-Band OFDM Physical Layer Proposal For IEEE 802.15 Task Group 3a”, November 2003.
 36. A. Saleh, R. Valenzuela, “A Statistical Model for Indoor Multipath Propagation”, *IEEE Journal On Selected Areas In Communications*, Vol. SAC-5, No.2, pp. 128-137, 1987.
 37. John G. Proakis, *Digital Communications*, Mcgraw-Hill, 4-Th Ed., 2001.
 38. Q. Zou, A. Tarighat, A. H. Sayed, “Performance Analysis of Multiband OFDM UWB Communications with Application to Range Improvement”, *IEEE Transactions On Vehicular Technology*, Vol.56, No.6, Part 2, pp. 3864 - 3878, November 2007.
 39. Marvin K. Simon, Mohamed-Slim Alouini, *Digital Communication Over Fading Channels : A Unified Approach To Performance Analysis*, New York: Wiley, 2000.
 40. T. V. Ramabadran, S. S. Gaitonde, “A Tutorial on CRC Computations”, *IEEE Micro*, Vol.8, No.4, pp. 62-75, August 1988.